

## Referee 1

We thank the referee for a positive assessment of our manuscript. The comments (in black), our response (in blue) and changes to the manuscript (in red) are listed below.

R. Dörich and co-workers have presented convincing laboratory evidence that iodide-CIMS instruments efficiently detect HNO<sub>3</sub> as NO<sub>3</sub><sup>-</sup> but ONLY in the presence of ozone (which converts I<sup>-</sup> into IO<sub>x</sub><sup>-</sup> ions, which in turn react with HNO<sub>3</sub>). This finding has substantial implications for field studies using such instruments, and suggests that some previous measurements have been incorrectly interpreted. This is one more example of how the powerful tool of chemical ionisation should be used very carefully, with due consideration of possible side reactions, including indirect pathways such as that discovered here. The study is definitely worth publishing in AMT. I have only very minor corrections and questions as described below.

-On line 135, reaction (R6) should presumably be reaction (R7), i.e. I<sup>-</sup> + HNO<sub>3</sub> not I<sup>-</sup> + H<sub>2</sub>O.

Correction made

-On line 153, the product should presumably be IO<sub>3</sub><sup>-</sup> not IO<sub>2</sub><sup>-</sup>.

Correction made

-Line 159: Maybe mention already here the the O<sub>2</sub> concentration in the quoted studies was MUCH less than that in the atmosphere (or in these measurements) - I had a hard time reconciling the dominance of IO<sub>3</sub><sup>-</sup> with the stated rate coefficients, since I kept assuming 0.2 atm O<sub>2</sub>. Also, is it the lack of an IO<sub>3</sub><sup>-</sup> + O<sub>2</sub> reaction that drives the equilibrium toward IO<sub>3</sub><sup>-</sup> ? We now mention that the O<sub>2</sub> concentrations were ~4x that of O<sub>3</sub>. The question of what changes the equilibrium concentrations of IO<sub>x</sub> in our system is addressed later in the manuscript.

With the O<sub>3</sub> (~1-5 × 10<sup>10</sup> molecule cm<sup>-3</sup>), O<sub>2</sub> concentrations (~4 × that of O<sub>3</sub>) and reaction times used in these studies...

Could the authors use e.g. gas-phase acidity / proton affinity data to estimate thermodynamic parameters (at least endo/exothermicity) for reactions R13-R15 (and also R19-R21)?

We have add some information regarding thermodynamic properties for the “new” reaction of IO<sub>x</sub><sup>-</sup> with HNO<sub>3</sub>:

Using heats of formation (in kJ mol<sup>-1</sup> at 298 K) of ΔH<sub>f</sub>(IO<sub>3</sub><sup>-</sup>) = -211 (Eger et al., 2019), ΔH<sub>f</sub>(HNO<sub>3</sub>) = -134 (Goos et al., 2005), ΔH<sub>f</sub>(HOIO<sub>2</sub>) = -95 (Khanniche et al., 2016) and ΔH<sub>f</sub>(NO<sub>3</sub><sup>-</sup>) = -312 (Goos et al., 2005) we calculate that reaction R15 is exothermic by ~62 kJ mol<sup>-1</sup>.

The reactions listed in R19-R21 are well known and documented as CIMS detection schemes; in this case the addition of thermodynamic properties is not necessary.

Could the authors speculate about the reasons for the differences in rate coefficients for reactions R13...R15? The ion size seems to play a role, but is that enough to explain a difference of a factor of 3 between IO<sup>-</sup> and IO<sub>3</sub><sup>-</sup>?

We state that “The results indicate qualitatively that IO<sub>3</sub><sup>-</sup> is the most reactive of the IO<sub>x</sub><sup>-</sup> anions towards HNO<sub>3</sub>, but that all three contribute to HNO<sub>3</sub> detection.” As the referee states, ion-size may play a role but there will be other factors. Given the assumptions made in deriving these “approximate” rate coefficients, and our lack of theoretical tools to examine ion-molecule reactions in detail, we feel that discussion of the apparent differences in rate coefficients is not appropriate.

-Line 221: “shut of” should be “shut off”

Correction made

## Referee 2

We thank the referee for a positive assessment of our manuscript. The comments (in black), our response (in blue) and changes to the manuscript (in red) are listed below.

This is a very nice manuscript that explores a large dynamic signal that occurs at mass to charge ratio 62 ( $\text{NO}_3^-$ ) in the iodide CIMS instruments. This signal has long puzzled users of the iodide ion for detection of trace gases, and this manuscript adds extremely valuable information to that ongoing debate. The manuscript is clearly written and organized and presents a well thought out convincing argument assigning signal at 62 to  $\text{HNO}_3$  detection via the  $\text{IO}_x^-$  anion. This will be a valuable addition to the existing literature on iodide CIMS and I fully support its publication pending minor changes.

It has been my own experience, having run a similar set of experiments, that addition of significant  $\text{O}_3$  to the iodide CIMS instrument while holding  $\text{HNO}_3$  addition constant will result in observable depletion of  $\text{IHNO}_3^-$  observed at  $m/z$  190, even when normalizing to iodide. The authors convey nicely that the impact of ozone on signal detection will be highly variable depending on the instrumental conditions used, and that alone could be the difference here.

However, considering the authors present  $\text{HNO}_3$  data from the field using observations at  $m/z$  190, the data should exist from the laboratory experiments to validate that this does not occur in their system. It would be beneficial to this manuscript if the authors could include a figure similar to 7a but looking at the signal at  $m/z$  190. This information is important to validate some of the assumption throughout the manuscript such as on page 8, line 232 where it is indicated that “negligible depletion of  $\text{HNO}_3$ ” occurs, a fully testable assumption considering the ability to detect  $\text{HNO}_3$  at  $m/z$  190. It would also be useful in understanding the comparisons of the  $m/z$  62 and  $m/z$  190 data at the end of the manuscript from the ambient observations.

In summary, the referee asks whether the  $\text{HNO}_3$  mixing ratio in the IMR (and thus its detection at  $m/z$  190) is influenced by the addition of  $\text{O}_3$ . We have conducted laboratory experiments in which a constant flow of  $\text{HNO}_3$  was monitored at  $m/z$  62 and  $m/z$  190 while various amounts of  $\text{O}_3$  (up to 800 ppbv) were added. The results are now displayed as a new Figure (8) and described in a new section (3.1);

### 3.2 Detection of $\text{HNO}_3$ at $m/z$ 190

We now compare the detection of  $\text{HNO}_3$  at  $m/z$  62 to its detection at  $m/z$  190, the  $\text{I}(\text{HNO}_3)$  adduct, with various amounts of  $\text{O}_3$  present. In Fig. 8 we present the results of an experiment in which a constant flow of  $\text{HNO}_3$  (12.5 ppbv) was introduced into the inlet and the ozone mixing ratio was varied from zero to 900 ppbv. We observe a great increase in the signal at  $m/z$  62 as expected (from 9 counts to > 6000 counts). At zero ozone, the signal at  $m/z$  190 is about 1000 counts and is largely background free, making this the preferred mass to monitor  $\text{HNO}_3$  in the absence of  $\text{O}_3$ . The cross-over point (when the signals at  $m/z$  62 and  $m/z$  190 are equal) is at an ozone mixing ratio of 100 ppbv. At an ozone mixing ratio of 800 ppbv, the signal at  $m/z$  62 is a factor 8.5 larger than that at  $m/z$  190.

Apparent from this figure is the depletion of the signal at  $m/z$  190 as the  $\text{O}_3$  mixing ratio increases to values of 800 ppbv, as observed e.g. in the lower stratosphere. The solid lines are least-squares fits to the datasets that describe the exponential growth of the  $m/z$  62 signal as  $\text{O}_3$  is increased and the exponential decay of  $m/z$  190 over the same range. The reduction in signal at  $m/z$  190 is characterised by an exponential term  $\exp(-0.00046 \times [\text{O}_3])$  which means that at 800 ppbv  $\text{O}_3$  a ~30% reduction in sensitivity is observed. The loss of sensitivity at  $m/z$  190 is driven by the loss of  $\text{I}^-$  in the IMR as  $\text{O}_3$  is added. At the same time, the depletion of the signal at  $m/z$  127 is weaker, which reflects the fact that only a small fraction of  $\text{IO}_x^-$  formed in

the IMR are detected, the rest presumably being fragmented in the CDC before being detected as I.

The fact that some I is converted to IO<sub>x</sub> in the IMR at high O<sub>3</sub> levels but is not reflected in the I signal at *m/z* 127 has repercussions for normalisation of product ion signals to the primary ion signal whereby the assumption is made that the measured signal at *m/z* 127 stems only from I. In our instrument, the loss of I in the IMR is significant at high levels of O<sub>3</sub> (e.g. 30 % at 800 ppbv O<sub>3</sub>). For this reason, we normalise the signals using values of the signal at *m/z* 127 obtained by interpolating between measurements obtained when scrubbing the air. The normalisation problem may occur in other I-CIMS instruments to varying extents, and the degree of bias will depend on the conversion of I<sup>-</sup> to IO<sub>x</sub><sup>-</sup> and the extent to which IO<sub>x</sub><sup>-</sup> is detected as I. The potential bias can be circumvented by the continuous addition of a calibration gas that is detected via reaction with I.

We have modified text in other positions. On page 5 we now write:

Throughout the paper, when presenting raw data, we generally normalise the I-CIMS signal by dividing by the primary ion signal at *m/z* 127. This is standard practise and corrects for drifts in the CH<sub>3</sub>I flow which may occur over several hours after the instrument was switched from standby mode to operational mode. It also accounts for longer term drifts caused by the weakening activity of the <sup>210</sup>Po source over the duration of a measurement campaign (months) or since the last calibration and for loss of detector sensitivity over similar time periods. We show later, that when adding large concentrations of reactants that significantly deplete the primary ion signal at *m/z* 127 this procedure may lead to bias in some measurements. For this reason, when detecting HNO<sub>3</sub> at *m/z* 190 (see later), we normalise to an interpolated signal at *m/z* 127 that was measured when the air was scrubbed.

In the abstract we now write:

At high ozone mixing ratios, we show that the concentration of I ions in our IMR is significantly depleted. This is not reflected by changes in the measured I signal at *m/z* 127 as the IO<sub>x</sub><sup>-</sup> formed do not survive passage through the instrument, but are likely detected after fragmentation to I. This may result in a bias in measurements of trace gases using I-CIMS in stratospheric air masses unless a calibration gas is continuously added or the impact of O<sub>3</sub> on sensitivity is characterised.

Figure 10 (now 11) has been modified to take the O<sub>3</sub> dependence of the sensitivity to HNO<sub>3</sub> at *m/z* 190 into account.

I am having a difficult time understanding how the authors are able to retrieve an ambient HNO<sub>3</sub> signal from the NO<sub>3</sub><sup>-</sup> signal. The signal that occurs at that mass is dependent on a changing HNO<sub>3</sub> ambient concentration as well as a changing O<sub>3</sub> concentrations. It would seem rather difficult to retrieve the real concentration unless you make an assumption that at any given point HNO<sub>3</sub> is not changing and only O<sub>3</sub> is changing, or the other way around. The only way this may work is if the authors used a measurement of true O<sub>3</sub> collected during the ambient flights, however it is unclear from the description that this was the case, perhaps those details are just missing. If an ozone measurement was used what instrument provided that data. I would like to see more details of how the concentration profiles in Figures 9 and 10 are determined, and what assumptions were made. If the author agree that one can not retrieve true HNO<sub>3</sub> unless a true ozone measurement is used it would benefit the readers to explicitly state this. It is possible that a reader could interpret the data presented here to mean that by using the Iodide CIMS measure of IO<sub>x</sub><sup>-</sup> and NO<sub>3</sub><sup>-</sup> one can quantitatively measure HNO<sub>3</sub>.

It is, of course, correct that HNO<sub>3</sub> can only be derived from the signal at *m/z* 62 if O<sub>3</sub> (and H<sub>2</sub>O) are simultaneously measured. However, these parameters are essential to analysis of

atmospheric composition and are measured routinely in the HALO aircraft. We now mention this in the manuscript.

During both HALO campaigns, O<sub>3</sub> and H<sub>2</sub>O (required for analysis of the signal at  $m/z$  62) were routinely measured.

I am in general surprised by the lack of instrument response to ambient features in the data in figures 9, 10 and S1. HNO<sub>3</sub> should have a significant inlet response time relative to O<sub>3</sub> in the CIMS regardless of the inlet conditions. In figure S1 in particular there appears to not be any lag in the observations. This quality in addition to the exact correlation to O<sub>3</sub> makes me believe that you are really just detecting HNO<sub>3</sub> that is made inside of the instrument. Otherwise, I would expect some deviation between the ambient O<sub>3</sub> and HNO<sub>3</sub> from 12:00 to 15:00 in figure S1. Can the authors comment on the time response of their measurements? What does a laboratory time response on  $m/z$  190 look like relative to  $m/z$  62?

An examination of Figure 9 (blue O<sub>3</sub> curve in panel a and red  $m/z$  62 curve in panel b) shows that features (e.g. in O<sub>3</sub>) are matched by those in  $m/z$  62. The “time lag” which the referee refers to presumably relates to the sticky nature of HNO<sub>3</sub> on inlet material and might be expected to occur (to an extent depending on the inlet material and temperature) if the HNO<sub>3</sub> and O<sub>3</sub> were both ambient. We agree with the statement that the dominant contribution to the signal at  $m/z$  62 is from the polonium source, and we clearly show this in Figure 9. We do not try to disguise this fact and state that (because of this) the  $m/z$  62 data is not accurate and should not be overinterpreted. Comparison with the time-response of a laboratory source of HNO<sub>3</sub> is not helpful in this regard as we cannot conduct lab experiments under flight conditions using the HALO-trace-gas-inlet.

Has the data from Figure 10b been corrected for scrubber zeros? Is this actually signal over zero. The way the data correction is explained for 9b where an approximate exponential of the Po HNO<sub>3</sub> source is subtracted out would suggest that there are not real zeros removed from the ambient data, which would include source HNO<sub>3</sub>. If real zeros have not been used how do you know any of the features shown in figure 9b or 10b are real ambient signals. If real zeros were used why didn't they account for the Po source background?

The data presented in figure 10b has not been corrected for background HNO<sub>3</sub> from the Polonium source. This is not possible as scrubbing also removes O<sub>3</sub> and thus the signal from HNO<sub>3</sub> generated in the polonium source would also be (falsely) zeroed. We now clarify this and write:

We note that the background signal at  $m/z$  62 that originates from the polonium source cannot be obtained by scrubbing the air of HNO<sub>3</sub> as this also removes O<sub>3</sub> and thus also sensitivity to HNO<sub>3</sub> at this mass.

This ion chemistry is ultimately a three-body reaction as indicated in page 7, line 216. Therefore, the result should be quite dependent on IMR pressure. The iodide CIMS literature is filled with instruments running across a very large range of pressures, sometimes exceeding 100 mbar, do the authors have any data or comments on the impact of pressure on this ionization mechanism.

On page 7, line 16 we listed a NET reaction sequence in which three molecules are involved in sequential, bimolecular reactions. This is not to be confused with a termolecular (3-bodied reaction) in which pressure (i.e. collision rates) plays a role in quenching adducts that are initially formed with some degree of internal excitation. There is no reason to assume that the chemistry we outline is pressure dependent. In any case, as our objective was to understand the signals obtained during the HALO campaigns, we only conducted experiments at our “standard” airborne IMR pressure.

The authors comment on the potential issues with past data sets using iodide CIMS to measure PAN, due to the secondary acetate ion chemistry that is occurring. It is my experience that many if not all of the airborne systems employ a constant standard addition of  $^{13}\text{C}$  PAN to the instrument. I believe that this addition would account for any secondary ion loss due to IO<sub>x</sub>-chemistry. I think the authors should add a comment in their discussion on this point on pages 9/10. While there are likely many dataset that have not used such an internal standard to track sensitivity changes it is not appropriate to question the data set that have used that method. A related question is do the authors believe such a system would indeed correct for these ion chemistry issues? That could be a good couple sentence discussion to add here.

The referee is correct in stating that a continuous, internal  $^{13}\text{C}$  standard will avoid this problem (assuming that labelled acetate anions reacts with the same rate coefficient as the unlabelled one). We have amended the text appropriately:

One way to avoid this problem is the continuous addition of isotopically labelled PAN to the inlet (see e.g. Roiger et al. (2011)) as the secondary, reactive losses of  $^{12}\text{C}$  and  $^{13}\text{C}$   $\text{CH}_3\text{CO}_2^-$  are expected to be identical.

And also the abstract:

The loss of  $\text{CH}_3\text{CO}_2^-$  via conversion to  $\text{NO}_3^-$  in the presence of  $\text{HNO}_3$  may represent a significant bias in I-CIMS measurements of PAN and  $\text{CH}_3\text{C}(\text{O})\text{OOH}$  in which continuous calibration (e.g. via addition of isotopically labelled PAN) is not carried out.

On page 12, line 369 the authors state that 190 does not show any correlation with O<sub>3</sub>. However, in the same figure, #10, it is clear that 190 correlates with m62. It was previously argued in describing figure 9, using panel C that it is expected that HNO<sub>3</sub> should correlate with O<sub>3</sub> even after correction for this unique ion chemistry. Additionally, there are clearly features in 10b that correlate with the ozone signal shown in 10a. Please elaborate on the disagreement between these two statements.

The statement was ambiguous as correlation can be caused both by the expected covariance of stratospheric HNO<sub>3</sub> and O<sub>3</sub> but (for  $m/z$  62) also stems from the strong dependence of the sensitivity to HNO<sub>3</sub> on the O<sub>3</sub> mixing ratio at this mass. We now write:

Similar to the CAFE-Africa data-set, the signal at  $m/z$  62 covaries strongly with the O<sub>3</sub> mixing ratios, which were between ~40 and ~700 ppbv whereas the raw signals at  $m/z$  62 and  $m/z$  190 (both due to HNO<sub>3</sub>) bear little resemblance to each other.

On page 6 there is a discussion on the residence time in the flow tube and comparison to similar work. I encourage the authors to reconsider their calculation of the residence time in their flow tube as presented. With a critical orifice on a cylinder there will be a jetting effect of the air through the region such that your reaction timescale will not be equivalent to the laminar sweeping of the volume. Rather it will be dependent on the velocity and flow dynamics of that jetting effect. This likely results in a significantly shorter reaction time than the volumetric calculation for most of the analyte molecules being sampled. It is not necessarily a discussion that is needed here but should be considered when trying to understand the difference being discussed, and leveraged as a potential answer for some of the disagreement observed.

Agreed. We do not know the flow-dynamic in the IMR and now emphasise that the reaction times are rough approximations. We write:

Note that the IMR reaction times we derive are only approximate as we do not take into account the mixing and flow dynamics in the IMR, which are likely to be complex (and possibly shorter than 25 ms) owing to sampling via a critical orifice. While we can not rule out that our observation of IO<sup>-</sup> (and not IO<sub>3</sub><sup>-</sup>) being the dominant ion-signal is partially caused by differences in reaction times, slight differences in O<sub>3</sub> concentrations and differences in temperature (our IMR is at ~15°C above ambient temperature owing to the heated inlet) we note that the higher pressure of O<sub>2</sub> (factor ~1-10 × 10<sup>4</sup>) in our IMR is likely to have a large effect.

Figure 1. I am interested in the flow dynamics in the figure with the initial sampling line. It appears that at some point your inlet could be connected to a pump exhaust line in the far left of the diagram. Even if overflowing the inlet with N<sub>2</sub>, depending on the flow characteristics and pressures I could see a scenario where pump exhaust would flow out the inlet past your sampling point. Perhaps something is missing or I am interpreting this diagram incorrectly.

When overflowing with line with N<sub>2</sub> a valve is closed and the connection to the exhaust line is closed. We have added this information to the caption.

When overflowing the inlet line, the valve to the exhaust line is closed. When sampling air, the valve to the N<sub>2</sub> bottle is closed.

Why do the authors believe the HNO<sub>3</sub> to 62 appears nonlinear in the inset figures on Fig 2 and 8?

We are dealing with very small signals when either acetate anion or O<sub>3</sub> are absent. The signal is close to background levels and may be influenced by variations therein. The point of the expanded scale in the insets is just to show that the signal is very low and detection of HNO<sub>3</sub> very inefficient.

Figure 9 and 10. These figures are difficult to interpret because there is not legend given in the figure and the colors are reused for different species. In 9, I believe the label attitude should be black and without reading the caption the reader has no idea what the pink line is for example. Blue is used in 3 places in Fig 9 for three different things.

Figure 9 (now 10) has been redrawn with more legends and corrected colours. Figure 10 (NO<sub>2</sub> 11) has also been redrawn and the lines better defined.

Page 8, line 238 needs a space between the and IOx

Correction made

Page ,8, line 241, suggest adding the word “of” in front of 100 greater.

Correction made

Page 9, line 265, there is a close parenthesis missing.

Correction made

Page 12, line 371, calibrations should be singular

Correction made

### Referee 3

We thank the referee for a positive assessment of our manuscript. The comments (in black), our response (in blue) and changes to the manuscript (in red) are listed below.

The paper reports an investigation of the influence of the presence of HNO<sub>3</sub> on the detection of NO<sub>3</sub><sup>-</sup> and N<sub>2</sub>O<sub>5</sub> when using chemical ionization mass spectrometry with I<sup>-</sup> as the reactant ion. Investigations are reported for especially the effect of ozone and humidity (that may affect the reactions through direct association of water molecules to ions). Additionally, the effect of PAN or PAA, that can release acetate anions causing extra reactions with HNO<sub>3</sub>, are reported. Finally, examples of field data, where the significance of the HNO<sub>3</sub> trace gas is important for data interpretations of I-CIMS data, is given. The reported investigations were motivated by observations from airborne measurements using an I-CIMS where the magnitude and variation of the signal at mass 62 (NO<sub>3</sub><sup>-</sup>) seemed to contradict previous beliefs on the measurement sensitivity to trace amounts of HNO<sub>3</sub>.

The theme of systematic sources of inaccuracies in CIMS measurements is of high relevance in general to atmospheric measurements and the presented results give important information on this aspect for the particular case of HNO<sub>3</sub> trace gases in I-CIMS. As such the paper is of high relevance.

The supplementary information is not available, and as I learned from the editors, this information was actively removed by the authors prior to the review process. The supplementary information is in fact heavily needed to critically address the content of the paper, in particular

- Page 2 - Fig. S1 – should illustrate the data that motivated the re-investigation of the sensitivity of the I-CIMS detection of N<sub>2</sub>O<sub>5</sub> to presence of the HNO<sub>3</sub> trace gas
- Page 4 - Fig. S2 – should show details of the experimental calibration
- Page 9 - Fig. S3 – should give more information on the data corresponding in fig. 7
- Page 12 - Fig. S4 + Fig. S5 – should show data from The CAFE-Europa flights

I consider the removal of the supplementary information, where essential information is given and to which reference is made throughout the manuscript, as rather unserious and problematic. On this account, I would strongly hesitate to consider the paper for acceptance.

We posted the SI in response to this comment. As we state, the retraction of the SI was not intentional. If we had not intended to show the SI we would not have cited it in the manuscript.

General comments to the paper.

While the introduction is well written and easily accessible, the sections “experimental details” and “Laboratory characterization” could well be worked over again for logic argumentation and clarity in the presentation.

I have the following specific comments, if the editors at all find the paper relevant for publication after the removal of the supplementary information.

We posted the SI in response to this comment.

Comment 1: Title and Abstract (e.g. line 11,14). The meaning of PAN is not given. Should be mentioned the same way as PAA.

In line 14 either use PAN and PAA or give the chemical formulas for both – a least be consistent.

In the atmospheric chemistry community the acronym PAN is more readily recognised than its correct, full name (peroxy acetyl nitric anhydride) so we prefer to keep it as PAN in the title. However, we have now defined PAN in the abstract:

....in the presence of peroxy acetyl nitric anhydride (PAN) or peroxyacetic acid (PAA).... and subsequently refer to the acronyms....

The loss of  $\text{CH}_3\text{CO}_2^-$  via conversion to  $\text{NO}_3^-$  in the presence of  $\text{HNO}_3$  may represent a significant bias in I-CIMS measurements of PAN and PAA in which continuous calibration (e.g. via addition of isotopically labelled PAN) is not carried out.

Comment 2: Page 2, Line 34-45 – several references to literature is missing . The statement “In very well known series of reactions ...” must be backed up with a reference where one can find the reaction rate constants for these reactions.

We now list two citations:

In a very well-known series of reactions (Lightfoot et al., 1992; Atkinson et al., 2004), NO is oxidised (R1, R2) by reaction with  $\text{O}_3$  or peroxy radicals ( $\text{RO}_2$ ) to  $\text{NO}_2$

The statement on the “non-gas loss process” should also be backed by references

We now write:

Both  $\text{HNO}_3$  and  $\text{N}_2\text{O}_5$  have important, non-gas-phase loss processes (Crowley et al., 2010) such as uptake to particles and other surfaces.

The statement on rapid photolysis of  $\text{NO}_3$  should also be quantified with a reference and an actual number for the photolysis rate.

It is not possible to quote a single number for a photolysis rate without defining the solar zenith angle and cloud-cover. We prefer to state its approximate daytime lifetime and provide a citation.

The chain of reactions to form  $\text{N}_2\text{O}_5$  is broken during the day as  $\text{NO}_3$  is generally photolysed within a few seconds (Wayne et al., 1991)...

Comment 3: Page 3, line 81. I believe a rate of  $380 \text{ s}^{-1}$  would correspond to  $\sim 3 \text{ ms}$  rather than  $\sim 2 \text{ ms}$  as stated, or simply state  $2.63 \text{ ms}$  to keep the number of significant digits ?. I am also missing the reference that tells where the stated reaction rates comes from, i.e, where do the numbers  $380 \text{ s}^{-1}$  and  $1940 \text{ s}^{-1}$  come from.

As we quote only approximate temperatures, we prefer not to give an accurate lifetime w.r.t. thermal decomposition. We now provide citations and write:

At this inlet temperature and pressure, the lifetime of PAN with respect to thermal decomposition  $< 3 \text{ ms}$  (IUPAC, 2021). For  $\text{N}_2\text{O}_5$ , the lifetime with respect to its thermal dissociation to  $\text{NO}_2$  and  $\text{NO}_3$  is  $\sim 0.5 \text{ ms}$  (IUPAC, 2021)).

To appreciate the importance of these timescales, the authors should also specify the transport time of the various ions through the instruments sectors. I realize that some of this information can (partly) be reconstructed from the description of pages 6-7, but it should be clearly stated in this place, which would also ease the reading of the pages 6-7 a lot.

As this point of the manuscript we are dealing with the likelihood that PAN and  $\text{N}_2\text{O}_5$  are thermally decomposed in the heated inlet. The residence time for PAN and  $\text{N}_2\text{O}_5$  in the heated inlet is already stated on the preceding line of text. Adding text about residence times in the IMR is not appropriate here.

Comment 4: page 3, line 86. Give reference to the origin of the stated reaction rate constants.

A citation (to IUPAC) has been added:

As NO reacts more rapidly with  $\text{NO}_3$  than with  $\text{CH}_3\text{C}(\text{O})\text{O}_2$  at  $170 \text{ }^\circ\text{C}$  ( $k_{\text{NO}+\text{NO}_3} = 2.3 \times 10^{-11} \text{ cm}^3 \text{ molecule}^{-1} \text{ s}^{-1}$ ,  $k_{\text{NO}+\text{CH}_3\text{C}(\text{O})\text{O}_2} = 1.4 \times 10^{-11} \text{ cm}^3 \text{ molecule}^{-1} \text{ s}^{-1}$  (IUPAC, 2021))

What was the actual concentration of added NO ?

The concentration of NO is now listed:

...we periodically add NO ( $\sim 5 \times 10^{12}$  molecule  $\text{cm}^{-3}$ ) to the inlet to remove  $\text{CH}_3\text{C}(\text{O})\text{O}_2$  and thus eliminate sensitivity to PAN.

Comment 5: page 5, line 133. To appreciate that it is correct to normalize all signals to the primary ions signal, the reader need to be assured that the intensity of this peak (mass 127) is not affected (i.e. only marginally) by the reactions taking place. The authors needs to quantify this more precisely. I am in particular puzzled, since the  $[\text{I}(\text{H}_2\text{O})]/[\text{I}]$  ratio changes dramatically (approximately a factor of 7 (stated as 6, line 116)), so a least humidity must be important here. The loss of intensity at  $m/z$  127 is because water is present at much larger concentrations (percent in the boundary layer) than the trace-gases we try to detect (usually in the ppb range or lower). This is why the normalised signals are further corrected for relative humidity, as we describe. This is standard practice. We extend and clarify this:

Throughout the paper, when presenting raw data, we generally normalise the I-CIMS signal by dividing by the primary ion signal at  $m/z$  127. This is standard practise and corrects for drifts in the  $\text{CH}_3\text{I}$  flow which may occur over several hours after the instrument was switched from standby mode to operational mode. It also accounts for longer term drifts caused by the weakening activity of the  $^{210}\text{Po}$  source over the duration of a measurement campaign (months) or since the last calibration and for loss of detector sensitivity over similar time periods. We show later, that when adding large concentrations of reactants that significantly deplete the primary ion signal at  $m/z$  127 this procedure may lead to bias in some measurements. For this reason, when detecting  $\text{HNO}_3$  at  $m/z$  190, we normalise to an interpolated signal at  $m/z$  127 that was measured when the air was scrubbed.

We have also added a new Figure (8) and text (new section 3.2) related to the loss of I- (and thus sensitivity to  $\text{HNO}_3$ ) at  $m/z$  190 when adding large concentrations of  $\text{O}_3$  to the IMR.

**Comment 6: page 5, line 133-135.** Could you expand on the explanation why reaction R6 (association of water to I-) is affected by the concentration of  $\text{O}_3$ . This may be true in some indirect way, but to understand that, it really requires a more explicit explanation at this place in the paper.

Our apologies: The reference should have been to R7 and not to R6. We now write:

The weak signal in the absence of  $\text{O}_3$  (blue data points) confirms the conclusions of previous studies that derive a low rate coefficient for reaction (R7)

Comment 7: page 5, line 146. The statement “This could be confirmed ...  $m/z$  62” seems to reflect an action that the authors speculate could prove their point that the first mentioned explanation for the sensitivity to  $\text{O}_3$  is not likely. Is this speculation or did you really do the suggested measurement ? It would be good to see the suggested evidence. (A figure in the missing supplementary information would be fine)

We use “could” not in the sense of “might have been able to” but as the past tense of “can” i.e. “were able to”. To remove any ambiguity we now write:

This was confirmed by adding NO.....

Comment 8: page 5, R10. On the right hand side, IO2- should be IO3-

Correction made

Comment 9: page 6-7 - discussion of the observed intensities of IOx-

Given the rate coefficients of the various reactions, it seems straightforward to calculate the steady state distributions of I-, IO-, IO<sub>2</sub>-, and IO<sub>3</sub>- under the various conditions shown in figure 3. Following all the argument that ends on line 200, I believe it would worthwhile to do such a (simple) calculation and compare the result to the data in figure 3.

We considered this, but there are too many uncertainties including the reaction time, the greatly different rate coefficients presented in the two studies (Teiwes and Bhujel), the lack of information about the influence of water clusters, the potential impact of non-thermal reactions in these low-pressure studies and the possibility that we do not detect all IO<sub>x</sub>- anions with the same efficiency. The goal of the present study was not to elucidate details of the reactions of IO<sub>x</sub> anions but to show that 1) they are formed when O<sub>3</sub> is present and 2) that they are likely candidates for the observed detection of HNO<sub>3</sub>.

Moreover, following the discussion one page 7-8, in line 242, the statement is made that “confirming that the detection of IO<sub>3</sub>- in our experiment is inefficient” (see also line 223-24). I am puzzled if the efficiencies of the various IO<sub>x</sub>- components may affect the actual relative intensity ratios between them. The authors need to clarify this issue.

We state that:

“However, the relative ion-abundance we observe at the detector does not necessarily reflect the relative concentration of the ions in the IMR and we cannot assign the individual contribution of any single IO<sub>x</sub><sup>-</sup> anion to HNO<sub>3</sub> detection.”

This states clearly that we know neither the absolute numbers nor the relative abundance of IO<sub>x</sub>- in the IMR. Given the uncertainties listed in the reply to the comment above, it is not obvious how we can further clarify this. We now weaken this statement by writing:

We note that the increase in signal at *m/z* 62 is about a factor of 100 greater than the reduction in the signal from IO<sub>x</sub><sup>-</sup>, IMPLYING that the detection of IO<sub>3</sub><sup>-</sup> in our instrument is inefficient.

Comment 10: figure 7a and equation 2. Please explain the idea of suggesting the form in equation 2 to represent the data. I suppose it represents a sort of saturation – but please clarify this more explicitly. Also the description in line 251 that “is clearly non-linear” is not really true: except for the lowest curve (18.5ppbv) all displayed curves are in fact linear to a good approximation as also suggested by eqn. 2, which is indeed almost linear at low [O<sub>3</sub>].

The amount of IO<sub>x</sub> anions formed depends exponentially on the rate coefficient (*k*), the concentration [O<sub>3</sub>] of ozone in the IMR and the reaction time (*t*): [IO<sub>x</sub>]*t* = [I]<sub>0</sub>(1-exp[-*k*[O<sub>3</sub>]*t*]).

This is why we chose this form of equation.

After equation 2 we have added:

Which reflects the expected exponential dependence of the concentration of IO<sub>x</sub><sup>-</sup> in the IMR on the O<sub>3</sub> concentration.

# Iodide-CIMS and $m/z$ 62: The detection of $\text{HNO}_3$ as $\text{NO}_3^-$ in the presence of PAN, peroxyacetic acid and ozone

Raphael Dörich,<sup>1</sup> Philipp Eger,<sup>1</sup> Jos Lelieveld<sup>1</sup> and John N. Crowley.<sup>1</sup>

5 <sup>1</sup>Atmospheric Chemistry Department, Max Planck Institute for Chemistry, 55128, Mainz, Germany

*Correspondence to:* John N. Crowley (john.crowley@mpic.de)

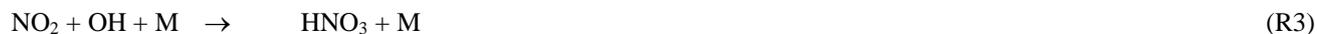
**Abstract.** Chemical Ionisation Mass Spectrometry (CIMS) using  $\text{I}^-$  (the iodide anion) as primary reactant ion has previously been used to measure  $\text{NO}_3$  and  $\text{N}_2\text{O}_5$  both in laboratory and field experiments. We show that reports of the large daytime mixing ratios of  $\text{NO}_3$  and  $\text{N}_2\text{O}_5$  (both usually present in detectable amounts only at night) are likely to be heavily biased by the ubiquitous presence of  $\text{HNO}_3$  in the troposphere and lower stratosphere. We demonstrate in a series of laboratory experiments that the CIMS detection of  $\text{HNO}_3$  at  $m/z$  62 using  $\text{I}^-$  ions is efficient in the presence of peroxy acetyl nitric anhydride (PAN) or peroxyacetic acid (PAA) and especially  $\text{O}_3$ . We have characterised the dependence of the sensitivity to  $\text{HNO}_3$  detection on the presence of acetate anions ( $\text{CH}_3\text{CO}_2^-$ ,  $m/z$  59, from either PAN or PAA). The loss of  $\text{CH}_3\text{CO}_2^-$  via conversion to  $\text{NO}_3^-$  in the presence of  $\text{HNO}_3$  may represent a significant bias in I-CIMS measurements of PAN and PAA in which continuous calibration (e.g. via addition of isotopically labelled PAN) is not carried out. The greatest sensitivity to  $\text{HNO}_3$  at  $m/z$  62 is achieved in the presence of ambient levels of  $\text{O}_3$  whereby the thermodynamically disfavoured, direct reaction of  $\text{I}^-$  with  $\text{HNO}_3$  to form  $\text{NO}_3^-$  is bypassed by the formation of  $\text{IO}_x^-$ , which react with  $\text{HNO}_3$  to form e.g. iodic acid and  $\text{NO}_3^-$ . The ozone and humidity dependence of the detection of  $\text{HNO}_3$  at  $m/z$  62 was characterised in laboratory experiments and applied to daytime, airborne measurements in which good agreement with measurements of the  $\text{I}^-(\text{HNO}_3)$  cluster-ion (specific for  $\text{HNO}_3$  detection) was obtained. At high ozone mixing ratios, we show that the concentration of  $\text{I}^-$  ions in our IMR is significantly depleted. This is not reflected by changes in the measured  $\text{I}^-$  signal at  $m/z$  127 as the  $\text{IO}_x^-$  formed do not survive passage through the instrument, but are likely detected after fragmentation to  $\text{I}^-$ . This may result in a bias in measurements of trace gases using I-CIMS in stratospheric air masses unless a calibration gas is continuously added or the impact of  $\text{O}_3$  on sensitivity is characterised.

## 25 1 Introduction

The use of iodide anions ( $\text{I}^-$ ) as primary ions in mass-spectrometric studies of ion-molecule reactions has a long history. Fehsenfeld et al. (1975) and Davidson et al. (1978) established that the nitrate anion ( $\text{NO}_3^-$ ,  $m/z$  62) was formed in a rapid reaction between  $\text{I}^-$  and  $\text{N}_2\text{O}_5$ .  $\text{NO}_3^-$  was also identified as the main product of the reaction between  $\text{I}^-$  and  $\text{ClONO}_2$  (Huey et al., 1995). The large rate constants for reaction of  $\text{I}^-$  with  $\text{N}_2\text{O}_5$  and  $\text{ClONO}_2$  led to the development of Chemical Ionisation Mass Spectrometry (CIMS) using  $\text{I}^-$  primary ions (henceforth I-CIMS) in kinetic studies of heterogeneous, atmospheric

reactions (e.g. (Hanson and Ravishankara, 1991)) and more recently has found widespread deployment for measurement of atmospheric trace gases ((Huey (2007) and references therein). Early field measurements utilised I-CIMS to detect N<sub>2</sub>O<sub>5</sub> and peroxyacetyl nitric anhydride (PAN, CH<sub>3</sub>C(O)O<sub>2</sub>NO<sub>2</sub>) (Slusher et al., 2004) but since then the range of molecules that have been detected using I has greatly increased and trace-gases as diverse as inorganic radicals and halogenates and a host of organic species are now routinely measured (Huey, 2007; Lee et al., 2014; Iyer et al., 2017; Riva et al., 2019). In this work, we focus on the detection of two atmospherically important trace gases N<sub>2</sub>O<sub>5</sub> and HNO<sub>3</sub> using a CIMS operating with I reactant ions.

Both N<sub>2</sub>O<sub>5</sub> and HNO<sub>3</sub> are formed in the atmosphere by the sequential oxidation of NO, which has both anthropogenic and natural sources. In a well-known series of reactions (Lightfoot et al., 1992; Atkinson et al., 2004), NO is oxidised (R1, R2) by reaction with O<sub>3</sub> or peroxy radicals (RO<sub>2</sub>) to NO<sub>2</sub>, which during the day, may be removed by reaction with OH to form HNO<sub>3</sub> (R3) and during the night to form N<sub>2</sub>O<sub>5</sub> (R4, R5).



Both HNO<sub>3</sub> and N<sub>2</sub>O<sub>5</sub> have important, non-gas-phase loss processes (Crowley et al., 2010) such as uptake to particles and other surfaces. In addition, N<sub>2</sub>O<sub>5</sub> can thermally dissociate back to NO<sub>3</sub>.

The chain of reactions to form N<sub>2</sub>O<sub>5</sub> is broken during the day as NO<sub>3</sub> is generally photolysed within a few seconds (Wayne et al., 1991) and also reacts with NO so that N<sub>2</sub>O<sub>5</sub> is expected to be present at significant levels only at night-time.

The detection of N<sub>2</sub>O<sub>5</sub> using I reactant ions can be achieved by monitoring either the NO<sub>3</sub><sup>-</sup> product at *m/z* 62 (see above) or the adduct ion at *m/z* 235 (Kercher et al., 2009). The former is reported to be more sensitive and less dependent on water vapour concentrations but less specific, with large and highly variable background signals potentially arising from trace gases such as NO<sub>3</sub>, ClONO<sub>2</sub> and BrONO<sub>2</sub>. Despite this, night time N<sub>2</sub>O<sub>5</sub> has been monitored in ambient air (as NO<sub>3</sub><sup>-</sup>) using I reactant ions, showing reasonable agreement with optical methods (Slusher et al., 2004; Dubé et al., 2006; Chang et al., 2011).

During a recent, airborne deployment of our I-CIMS, we monitored NO<sub>3</sub><sup>-</sup> at *m/z* 62 in an attempt to detect N<sub>2</sub>O<sub>5</sub> during two night-time flights. The air masses we investigated were mainly in the tropical free and upper troposphere and lower stratosphere and we did not expect significant interference from e.g. halogen nitrates at *m/z* 62. However, our airborne measurements (described in detail in section 4) revealed a large and variable signal at *m/z* 62 during both the day and night. To illustrate this, raw signals obtained during daytime when the aircraft sampled air masses with varying degrees of stratospheric influence are displayed in Fig. S1. The signal at *m/z* 62 is large and highly variable and is not affected by addition of NO to the heated inlet, ruling out its assignment to either N<sub>2</sub>O<sub>5</sub> or NO<sub>3</sub> (see below). The great increase in signal

when entering the lower stratosphere and the obvious correlation with O<sub>3</sub> (Fischer et al., 1997; Popp et al., 2009) provided an early clue to the identity of the trace-gas detected at  $m/z$  62 which we initially assigned to HNO<sub>3</sub>. Our results thus appeared to contrast the conclusions of a previous observation of a large daytime signal at  $m/z$  62 when deploying an I-CIMS (in this case in the boundary layer), which was interpreted as resulting (at least in part) from high levels of daytime NO<sub>3</sub> and/or N<sub>2</sub>O<sub>5</sub> (Wang et al., 2014). Based on complementary laboratory experiments, Wang et al. (2014) showed, in accord with earlier investigations (Fehsenfeld et al., 1975; Huey et al., 1995), that HNO<sub>3</sub> is not detected sensitively at  $m/z$  62 using I-CIMS.

The unexpected observation of a large daytime signal at  $m/z$  62 during airborne operation led us to perform a series of laboratory experiments to identify potential “interfering” trace gases at this mass-to-charge ratio when using I-CIMS. In contrast to the conclusions drawn from previous studies, our laboratory and airborne measurements show that, during daytime, the predominant contributor to  $m/z$  62 when sampling ambient air (in the presence of ozone) is likely to be HNO<sub>3</sub>.

## 2 Experimental details

The I-CIMS we used in our laboratory and airborne investigations (see Fig. 1) is similar to that described by Slusher et al. (2004) and Zheng et al. (2011) and was originally constructed in collaboration with Georgia Tech as a prototype instrument of the company THS (<http://thsinstruments.com>). It is essentially a hybrid of the instruments described by Phillips et al. (2013) and Eger et al. (2019), the former using a <sup>210</sup>Po ion source, the latter an electrical discharge source but with improved (digital) control of the MS settings enabling different mass-to-charge ratios to be monitored using different potentials for the collisional dissociation of cluster ions. For all the experiments described below, the <sup>210</sup>Po ion source was used to generate I<sup>-</sup> as this configuration has much better sensitivity for PAN, the main target trace gas during the deployment of the I-CIMS on the HALO aircraft (High Altitude Long range platform for atmospheric Observations). The set-up for PAN detection includes a heated inlet section (~170 °C, 100 mbar, residence time ~ 40 ms) to thermally dissociate PAN to CH<sub>3</sub>C(O)O<sub>2</sub> which subsequently reacts with I<sup>-</sup> to form the acetate anion (CH<sub>3</sub>CO<sub>2</sub><sup>-</sup>) which is detected at  $m/z$  59. At this inlet temperature and pressure, the lifetime of PAN with respect to thermal decomposition < 3 ms (IUPAC, 2021). For N<sub>2</sub>O<sub>5</sub>, the lifetime with respect to its thermal dissociation to NO<sub>2</sub> and NO<sub>3</sub> is ~0.5 ms (IUPAC, 2021)) so that N<sub>2</sub>O<sub>5</sub> is stoichiometrically converted to NO<sub>3</sub> and the instrument measures the sum of N<sub>2</sub>O<sub>5</sub> and NO<sub>3</sub> at  $m/z$  62. In order to separate PAN signals from those of peroxyacetic acid (CH<sub>3</sub>C(O)OOH, also detected as CH<sub>3</sub>CO<sub>2</sub><sup>-</sup> at  $m/z$  59) we periodically add NO (~ 5 × 10<sup>12</sup> molecule cm<sup>-3</sup>) to the inlet to remove CH<sub>3</sub>C(O)O<sub>2</sub> and thus eliminate sensitivity to PAN. As NO reacts more rapidly with NO<sub>3</sub> than with CH<sub>3</sub>C(O)O<sub>2</sub> at 170 °C ( $k_{\text{NO}+\text{NO}_3} = 2.3 \times 10^{-11} \text{ cm}^3 \text{ molecule}^{-1} \text{ s}^{-1}$ ,  $k_{\text{NO}+\text{CH}_3\text{C(O)O}_2} = 1.4 \times 10^{-11} \text{ cm}^3 \text{ molecule}^{-1} \text{ s}^{-1}$  (IUPAC, 2021)) the concentration of NO added is also sufficient to quantitatively titrate NO<sub>3</sub> to NO<sub>2</sub> and thus provides a measure of the “background” signal at  $m/z$  62 in the absence of NO<sub>3</sub> and N<sub>2</sub>O<sub>5</sub>.

During airborne operation on HALO, the dynamic pressure generated in a forward facing trace gas inlet (TGI) located on top of the aircraft (see Fig. 1) was used to create a flow of air through ¼ inch (OD) PFA tubing sampling at an angle of 90° to the flight direction. The ¼ inch tubing was attached to a ½ inch (OD) PFA tube attached to an exhaust plate at the underside

of the aircraft to create a fast “bypass” flow. The bypass flow was sub-sampled (again at 90° and by ¼ inch PFA tubing heated to 40°C) by the 1.4 L (STP) min<sup>-1</sup> flow into the I-CIMS. Sub-sampling twice at 90° to the flow was helpful in reducing the number of large particles (e.g. cloud droplets) that could enter the thermal dissociation inlet and IMR.

100 The thermal dissociation inlet of the I-CIMS is regulated to a pressure of 100 mbar, which results in a pressure in the ion-molecule reactor of 24 mbar. This way, a stable pressure in the thermal dissociation inlet and the Ion Molecule Reactor (IMR) was maintained at altitudes up to ~15 km. Prior to take off, the inlet line and TGI were flushed with nitrogen to prevent contamination by the high levels of pollutant trace gases at the airport. As described in Eger et al. (2019) negative ions exiting the IMR were declustered in passage through a collisional dissociation region (CDC, 0.6 mbar) before passing through an octopole ion-guide ( $6 \times 10^{-3}$  mbar) and a quadrupole for mass selection ( $9 \times 10^{-5}$  mbar) prior to detection using a  
105 channeltron.

I<sup>-</sup> ions were generated by combining flows of 4 cm<sup>3</sup> (STP) min<sup>-1</sup> CH<sub>3</sub>I/N<sub>2</sub> (400 ppmv) with 750 cm<sup>3</sup> (STP) min<sup>-1</sup> N<sub>2</sub> and passing the mixture through a 370 MBq <sup>210</sup>Po source. Under standard operating conditions (including airborne deployment), a constant amount of H<sub>2</sub>O was added to the IMR by flowing 50 cm<sup>3</sup> (STP) min<sup>-1</sup> N<sub>2</sub> (at 1 bar pressure) through a 30 cm length of water-permeable 1/8-inch tubing (Permapure) immersed in water. The 50 cm<sup>3</sup> (STP) min<sup>-1</sup> flow of N<sub>2</sub> acquires a  
110 relative humidity close to 100 % in transit through the tubing and is subsequently mixed with the dry N<sub>2</sub> flow and sample air. Under these conditions, the ratio of signals at *m/z* 145 (I(H<sub>2</sub>O)) to that at *m/z* 127 (I<sup>-</sup>) was 0.068. By comparison with calibration curves (see Fig S2 and associated text) this indicates an H<sub>2</sub>O concentration in the IMR of  $\sim 4 \times 10^{14}$  molecule cm<sup>-3</sup>. For laboratory tests, the amount of water in the IMR could be increased by reducing the pressure in the permeable tube (thus increasing the mole fraction of H<sub>2</sub>O) or set to zero by bypassing the humidifier.

115 Based on a (calculated) literature value for the free energy of formation of I(H<sub>2</sub>O)<sub>1</sub> of -6.1 kcal mol<sup>-1</sup> (Teiwes et al., 2019) we derive an equilibrium constant (at 298 K) of  $K_6 = 1.16 \times 10^{-15}$  cm<sup>3</sup> molecule<sup>-1</sup> for the formation and thermal dissociation of I(H<sub>2</sub>O)<sub>1</sub>



With an H<sub>2</sub>O concentration (in the IMR) of  $3.9 \times 10^{14}$  molecule cm<sup>-3</sup> this implies that the ratio  $[\text{I}(\text{H}_2\text{O})_1] / [\text{I}^-] = 0.45$ . Our  
120 measured ratio of signals at *m/z* 145 (I(H<sub>2</sub>O)) / *m/z* 127 (I<sup>-</sup>) was a factor ~6 lower, reflecting the fact that, even when the declustering potential is reduced to its minimum value, most I(H<sub>2</sub>O) ions do not survive the CDC region.

During extended operation of the CIMS, changes in sensitivity were captured by monitoring the primary ion signal (I<sup>-</sup> and its water cluster). Background signals at each of the mass-to-charge ratios monitored were obtained by passing the sampled air through a tubular scrubber (aluminium) filled with stainless-steel wool heated to 120 °C.

**3.1 Detection of HNO<sub>3</sub> at *m/z* 62: The role of ozone**

As described above, our observations of a clear correlation between *m/z* 62 and O<sub>3</sub> mixing ratios during the first HALO deployment of the I-CIMS strongly suggested that HNO<sub>3</sub> was the origin of the signal although previous experiments had shown that I<sup>-</sup> does not react with HNO<sub>3</sub> to form NO<sub>3</sub><sup>-</sup>. In order to determine the sensitivity of our I-CIMS to HNO<sub>3</sub> we constructed a permeation source in which a 20 cm<sup>3</sup> (STP) min<sup>-1</sup> flow of zero air was passed through a 1m length of PFA tubing (0.125 inch OD) which was formed into a coil and submerged in an aqueous solution of 65% HNO<sub>3</sub> held at 50°C. The permeation rate was determined by passing the 20 cm<sup>3</sup> (STP) min<sup>-1</sup> flow through an optical absorption cell and measuring the optical extinction at 185 nm where the absorption cross-section of HNO<sub>3</sub> is well known (Dulitz et al., 2018). For the I-CIMS calibration, the 20 cm<sup>3</sup> (STP) min<sup>-1</sup> output was dynamically diluted to generate a mixing ratio of between 5 and 50 ppbv. Based on uncertainties in the absorption cross-section (5%), the reproducibility of the optical measurement and the dilution factor, the uncertainty of the HNO<sub>3</sub> mixing ratio is estimated as 15 %.

Figure 2 shows the response of the I-CIMS at *m/z* 62 to addition of various amounts of HNO<sub>3</sub>. Throughout the paper, when presenting raw data, we generally normalise the I-CIMS signal by dividing by the primary ion signal at *m/z* 127. This is standard practise and corrects for drifts in the CH<sub>3</sub>I flow which may occur over several hours after the instrument was switched from standby mode to operational mode. It also accounts for longer-term drifts caused by the weakening activity of the <sup>210</sup>Po source over the duration of a measurement campaign (months) or since the last calibration and for loss of detector sensitivity over similar time periods. We show later that, when adding large concentrations of reactants that significantly deplete the primary ion signal at *m/z* 127, this procedure may lead to bias in some measurements. For this reason, when detecting HNO<sub>3</sub> at *m/z* 190 (see later), we normalise to an interpolated signal at *m/z* 127 that was measured when the air was scrubbed.

The weak signal in the absence of O<sub>3</sub> (blue data points) confirms the conclusions of previous studies that derive a low rate coefficient for reaction (R7). For comparison, approximate, relative sensitivities to PAN (*m/z* 59), N<sub>2</sub>O<sub>5</sub> (*m/z* 62) and HNO<sub>3</sub> (*m/z* 62), using this instrument are 1, 0.1 and 5 × 10<sup>-4</sup>, respectively. Indeed, as written below, reaction (R7) is endothermic by ~43 kJ mol<sup>-1</sup> (Goos et al., 2005).



In a further series of experiments, we measured the response of the I-CIMS to HNO<sub>3</sub> when adding O<sub>3</sub> to the zero-air. The results, also plotted in Fig. 2 (black symbols), indicate a factor ~250 increase in the signal at *m/z* 62 when ~500 ppbv ozone was added. There are two possible explanations for this observation. The first involves conversion of NO<sub>2</sub> impurity (that is present as a ~8 % impurity in the HNO<sub>3</sub> permeation flow) to NO<sub>3</sub> and N<sub>2</sub>O<sub>5</sub> (R1, R4, R5) which are subsequently detected. This can however be ruled out as the rate-limiting step in the formation of NO<sub>3</sub> is the slow reaction between NO<sub>2</sub> and O<sub>3</sub> with  $k_4 = 3.5 \times 10^{-17} \text{ cm}^3 \text{ molecule}^{-1} \text{ s}^{-1}$  at room temperature (Atkinson et al., 2004). The addition of 1000 ppbv O<sub>3</sub> (equivalent to a concentration of 2.4 × 10<sup>13</sup> molecule cm<sup>-3</sup>) would only convert an insignificant fraction of the NO<sub>2</sub> to NO<sub>3</sub> in

the ~40 ms reaction time available from the point of mixing to the IMR. **This was confirmed by adding NO (7.7 ppm) to the inlet which would remove any NO<sub>3</sub> (see above) and observing no change in the signal at *m/z* 62.**

160 The second explanation is that the presence of O<sub>3</sub> results in the generation of further reagent ions that can react with HNO<sub>3</sub>. Iodide anions are known to react with O<sub>3</sub>, leading, in a series of exothermic reactions, to the formation of iodate (Williams et al., 2002; Teiwes et al., 2018; Bhujel et al., 2020).



In this scheme, R8 is rate-limiting ( $k_8 \sim 1 \times 10^{-12} \text{ cm}^3 \text{ molecule}^{-1} \text{ s}^{-1}$  (Bhujel et al., 2020), whereas the further steps (R9-R10) in the sequential oxidation to iodate proceed with rate constants at least two orders of magnitude larger (Teiwes et al., 2018; Bhujel et al., 2020). IO<sup>-</sup> and IO<sub>2</sub><sup>-</sup> also react with O<sub>2</sub> to reform O<sub>3</sub>:



with rate coefficients of  $k_{11} = 3.2 \times 10^{-14} \text{ cm}^3 \text{ molecule}^{-1} \text{ s}^{-1}$  and  $k_{12} = 1.3 \times 10^{-14} \text{ cm}^3 \text{ molecule}^{-1} \text{ s}^{-1}$  (Bhujel et al., 2020). **With the O<sub>3</sub> (~1-5 × 10<sup>10</sup> molecule cm<sup>-3</sup>), O<sub>2</sub> concentrations (~ 4 × that of O<sub>3</sub>) and reaction times used in their studies** (Teiwes et al., 2018; Teiwes et al., 2019; Bhujel et al., 2020) IO<sub>3</sub><sup>-</sup> was observed to be the dominant form of IO<sub>X</sub><sup>-</sup>.

In the presence of water vapour, I<sup>-</sup> is also present as a hydrate I(H<sub>2</sub>O) (see above) for which, according to Teiwes et al. 175 (2019), the rate coefficient for reaction with O<sub>3</sub> (R13a, R13b) is a factor ~40 larger than  $k_8$  and results in the formation of IO<sub>2</sub><sup>-</sup> and I<sup>-</sup>:



As R8 is rate limiting, this implies an increase in the amount of e.g. IO<sub>3</sub><sup>-</sup> formed in the IMR in the presence of water. In most 180 regions of the troposphere and lower atmosphere ozone mixing ratios lie between 30 and >1000 ppbv. An ambient ozone concentration of 50 ppbv results in a concentration in the IMR of > 10<sup>10</sup> molecules cm<sup>-3</sup>. The large rate coefficients for R9 and R10 and the reactions of IO<sup>-</sup> and IO<sub>2</sub><sup>-</sup> with O<sub>2</sub> result in the rapid inter-conversion of I<sup>-</sup>, IO<sup>-</sup>, IO<sub>2</sub><sup>-</sup> and IO<sub>3</sub><sup>-</sup> which results (for a given RH and ozone concentration) in a quasi-equilibrium between IO<sub>X</sub><sup>-</sup> anions.

We explored the relevance of these reactions for our I-CIMS by carrying out a set of experiments in which varying amounts 185 of O<sub>3</sub> were added to the inlet and the mass-to-charge ratios corresponding to IO<sup>-</sup> (*m/z* 143), IO<sub>2</sub><sup>-</sup> (*m/z* 159) and IO<sub>3</sub><sup>-</sup> (*m/z* 175) were monitored; the results are depicted in Fig. 3.

First, we note that all three mass-to-charge ratios were indeed observed, but only under conditions where the CDC potential was set to the lowest value at which ions still reach the detector. The dependence of the various IO<sub>X</sub><sup>-</sup> anions on the O<sub>3</sub> mixing ratio is broadly as expected from the reaction scheme (R8-R12) listed above: The major contributor to IO<sub>X</sub><sup>-</sup> at low [O<sub>3</sub>] is IO<sup>-</sup>, 190 which is converted to IO<sub>2</sub><sup>-</sup> and IO<sub>3</sub><sup>-</sup> more efficiently as O<sub>3</sub> increases, while the total concentration of IO<sub>X</sub><sup>-</sup> increases

approximately linearly. At the maximum O<sub>3</sub> mixing ratio used (577 ppbv) there are (following dilution) 375 ppbv in the IMR, which translates to a concentration (at 24 mbar and ~298 K) of  $2.1 \times 10^{11}$  molecule cm<sup>-3</sup>. This O<sub>3</sub> concentration is comparable with those used by Teiwes et al. (2018) ( $\sim 1-4 \times 10^{11}$  molecule cm<sup>-3</sup>) or Bhujel et al. (2020) ( $\sim 4 \times 10^{10}$  molecule cm<sup>-3</sup>) in their ion-trap based, kinetic investigations of the formation of IO<sub>X</sub><sup>-</sup> when reacting I<sup>-</sup> with O<sub>3</sub>. Their observation that IO<sub>3</sub><sup>-</sup> is the dominant anion is however not consistent with our results, which indicate that IO<sub>3</sub><sup>-</sup> represents only ~35% of the total IO<sub>X</sub><sup>-</sup> signal. The relative abundance of each IO<sub>X</sub><sup>-</sup> depends not only on the O<sub>3</sub> concentration but also on the reaction time, which, for both Teiwes et al. (2018) and Bhujel et al. (2020) was between 10-100 ms. Based on the flow into the IMR, its volume (~50 cm<sup>3</sup>) and the pressure we calculate a similar residence time (for neutrals) of about 25 ms. We also considered the possibility that the application in our I-CIMS of a potential difference between the entrance and exit of the IMR (to optimise ion-transmission) could result in a significantly shorter IMR-residence time for ions. This was assessed by calculating the drift-velocity ( $V_d$ ) in the IMR from the electric field strength ( $E \sim 12$  Vm<sup>-1</sup>) and the ion mobility ( $\mu$ ).

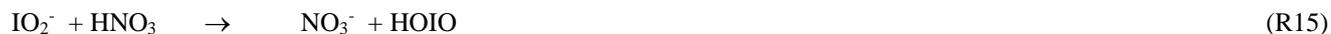
$$V_d = E\mu \quad (1)$$

The electrical mobility of I<sup>-</sup> was calculated for our conditions (using the Mason-Schamp equation) as  $\sim 0.15$  m<sup>2</sup> V<sup>-1</sup> s<sup>-1</sup> using a collision cross-section (for an I<sup>-</sup> / N<sub>2</sub> pair) of  $9 \times 10^{-16}$  cm<sup>2</sup> molecule<sup>-1</sup> (McCracken, 1952). Via equation (1), this results in a drift velocity of  $1.8$  m s<sup>-1</sup>, or an ion residence time (in the ~8 cm long IMR) of 44 ms, which is comparable to the residence time of neutrals. **Note that the IMR reaction times we derive are only approximate as we do not take into account the mixing and flow dynamics in the IMR, which are likely to be complex (and possibly shorter than 25 ms) owing to sampling via a critical orifice. While we cannot rule out that our observation of IO<sup>-</sup> (and not IO<sub>3</sub><sup>-</sup>) being the dominant ion-signal is partially caused by differences in reaction times, slight differences in O<sub>3</sub> concentrations and differences in temperature (our IMR is at ~15°C above ambient temperature owing to the heated inlet) we note that the higher pressure of O<sub>2</sub> (factor  $\sim 1-10 \times 10^4$ ) in our IMR is likely to have a large effect.** The presence of O<sub>2</sub> converts IO<sub>3</sub><sup>-</sup> back to IO<sup>-</sup> thus competing with further oxidation (via reaction with O<sub>3</sub>) to IO<sub>3</sub><sup>-</sup>. Additionally, the high IMR pressures (24 mbar) in our experiments are  $\sim$  six orders of magnitude higher than the  $\sim 10^{-5}$  mbar available in the ion-trap experiments of Teiwes et al. (2018) and Bhujel et al. (2020) which will result in more rapid thermalization of the ions present and prevent potentially non-thermal reactions and thus bias to the rate coefficients derived.

The effect of adding H<sub>2</sub>O to the IMR was explored in a further set of experiments and the variation of the signals at mass-to-charge ratios corresponding to IO<sub>X</sub><sup>-</sup> with [H<sub>2</sub>O] are displayed in Fig. 4. The experiments were carried out with the O<sub>3</sub> mixing ratio fixed at either 70 or 120 ppbv, close to that typically found in the lower troposphere (~20-100 ppbv). At the lowest H<sub>2</sub>O concentrations in our experiments, the total IO<sub>X</sub><sup>-</sup> signal is about 30 counts. This increases by a factor of  $\sim 10$  when [H<sub>2</sub>O]<sub>IMR</sub> increases to  $3 \times 10^{15}$  molecule cm<sup>-3</sup>. Increasing the O<sub>3</sub> mixing ratio from 70 to 120 ppbv results in an increase in the signals at  $m/z$  175 (IO<sub>3</sub><sup>-</sup>) and  $m/z$  159 (IO<sub>2</sub><sup>-</sup>) at all water vapour concentrations, whereas the signal at  $m/z$  143 (IO<sup>-</sup>) is reduced at the lowest water vapour concentrations. These observations reinforce the concept of a larger rate coefficient for reaction of

I(H<sub>2</sub>O) with O<sub>3</sub> (R13a) compared to I<sup>-</sup> (R8) (Teiwes et al., 2019) and the sequential conversion of IO<sup>-</sup> to more oxidized forms as described by equation R8-R10.

225 Having established that all of the expected IO<sub>X</sub><sup>-</sup> anions are present in our IMR, we can propose a route for HNO<sub>3</sub> detection as NO<sub>3</sub><sup>-</sup> which involves transfer of a proton from HNO<sub>3</sub> (a very strong acid) to the conjugate base of the respective iodine containing acids (hypoiodous-, iodous- and iodic-acid):



Taking IO<sub>3</sub><sup>-</sup> as an example, we see that the net reaction, (I<sup>-</sup> + O<sub>3</sub> + HNO<sub>3</sub> → NO<sub>3</sub><sup>-</sup> + HOIO<sub>2</sub>) is driven by the relative stability of iodic acid compared to O<sub>3</sub>, thus bypassing the thermodynamic barrier to direct formation of NO<sub>3</sub><sup>-</sup> from HNO<sub>3</sub> + I<sup>-</sup>. Using heats of formation (in kJ mol<sup>-1</sup> at 298 K) of ΔH<sub>f</sub>(IO<sub>3</sub><sup>-</sup>) = -211 (Eger et al., 2019), ΔH<sub>f</sub>(HNO<sub>3</sub>) = -134 (Goos et al., 2005), ΔH<sub>f</sub>(HOIO<sub>2</sub>) = -95 (Khanniche et al., 2016) and ΔH<sub>f</sub>(NO<sub>3</sub><sup>-</sup>) = -312 (Goos et al., 2005) we calculate that reaction R16

235 is exothermic by ~62 kJ mol<sup>-1</sup>.

As described above, the O<sub>3</sub> dependence of the ion signals we observe for IO<sup>-</sup>, IO<sub>2</sub><sup>-</sup> and IO<sub>3</sub><sup>-</sup> are consistent with the sequential oxidation of I<sup>-</sup> by O<sub>3</sub>. However, the relative ion-abundance we observe at the detector does not necessarily reflect the relative concentration of the ions in the IMR and we cannot assign the individual contribution of any single IO<sub>X</sub><sup>-</sup> anion to HNO<sub>3</sub> detection. We are unable to completely shut off collisional dissociation in our I-CIMS which may be a characteristic that is peculiar to our instrument as we do not detect weakly-bound I(R(O)OH) clusters which are commonly monitored in other instruments utilising I<sup>-</sup> chemical ionisation (Lee et al., 2014). Hence, our relative sensitivity to the IO<sub>X</sub><sup>-</sup> components is unknown.

In order to confirm that IO<sub>X</sub><sup>-</sup> is responsible for detection of HNO<sub>3</sub> we examined the depletion of the signals at *m/z* 143, *m/z* 159 and *m/z* 175 when adding very large concentrations of HNO<sub>3</sub> to the IMR. The results, summarised in Fig. 5, indicate that all three IO<sub>X</sub><sup>-</sup> ions are removed when the HNO<sub>3</sub> mixing ratio was increased from zero to 80 ppbv, but with different fractional changes. This can be understood if e.g. the individual IO<sub>X</sub><sup>-</sup> react with HNO<sub>3</sub> with different rate coefficients. The solid lines in Fig. 5 represent exponential decays of each ion, with rate coefficients of ~10 × 10<sup>-10</sup> cm<sup>3</sup> molecule<sup>-1</sup> s<sup>-1</sup> for HNO<sub>3</sub> + IO<sub>3</sub><sup>-</sup>, ~7 × 10<sup>-10</sup> cm<sup>3</sup> molecule<sup>-1</sup> s<sup>-1</sup> for HNO<sub>3</sub> + IO<sub>2</sub><sup>-</sup> and ~3 × 10<sup>-10</sup> cm<sup>3</sup> molecule<sup>-1</sup> s<sup>-1</sup> for HNO<sub>3</sub> + IO<sup>-</sup>. These approximate values were derived by converting the HNO<sub>3</sub> mixing ratio into a concentration in the IMR and assuming pseudo-first-order behaviour (i.e. negligible depletion of HNO<sub>3</sub>) so that (using IO<sub>3</sub><sup>-</sup> as example):

$$S(\text{IO}_3^-)_t = S(\text{IO}_3^-)_0 \exp(-kt[\text{HNO}_3]_{\text{IMR}})$$

Where S(IO<sub>3</sub><sup>-</sup>)<sub>t</sub> and S(IO<sub>3</sub><sup>-</sup>)<sub>0</sub> are the signals at *m/z* 175 after and prior to addition of HNO<sub>3</sub>, respectively. [HNO<sub>3</sub>]<sub>IMR</sub> is the concentration (molecule cm<sup>-3</sup>) of HNO<sub>3</sub> in the IMR, *k* (cm<sup>3</sup> molecule<sup>-1</sup> s<sup>-1</sup>) is the rate coefficient for reaction between HNO<sub>3</sub> and IO<sub>3</sub><sup>-</sup> and *t* is the reaction time, which we assume to be 25 ms (see above). This analysis assumes that the re-establishment of equilibria between IO<sub>X</sub><sup>-</sup> is minimal on the time scale of the reaction between any single IO<sub>X</sub><sup>-</sup> and HNO<sub>3</sub>. The results

255

indicate qualitatively that  $\text{IO}_3^-$  is the most reactive of the  $\text{IO}_x^-$  anions towards  $\text{HNO}_3$ , but that all three contribute to  $\text{HNO}_3$  detection. The depletion of the summed  $\text{IO}_x^-$  signals versus the accompanying increase in signal due to  $\text{NO}_3^-$  at  $m/z$  62 is displayed in Fig. 6, which indicates a roughly linear relationship, confirming that  $\text{IO}_x^-$  are mainly responsible for detection of  $\text{HNO}_3$  in our I-CIMS. We note that the absolute increase in signal at  $m/z$  62 is about a factor of 100 greater than the reduction in the signal from  $\text{IO}_x^-$ , implying that the detection of  $\text{IO}_3^-$  in our instrument is inefficient.

While the reactions of  $\text{IO}_x^-$  with  $\text{HNO}_3$  represent the most likely route to  $\text{HNO}_3$  detection at  $m/z$  62 in our CIMS other possibilities are the reactions of oxide, superoxide and ozone anions ( $\text{O}_x^-$ ) and hydrated  $\text{O}_x^-$  with  $\text{HNO}_3$  as they have large rate coefficients ( $> 10^{-9} \text{ cm}^3 \text{ molecule}^{-1} \text{ s}^{-1}$ ) and form  $\text{NO}_3^-$  (Huey, 1996; Wincel et al., 1996; Lengyel et al., 2020):



However, when adding  $\text{O}_3$  (up to 600 ppbv) to the IMR we saw no signal that could be attributable to any oxide anion  $\text{O}_x^-$ .

Figure 7a displays the dependence of the  $\text{NO}_3^-$  signal at  $m/z$  62 on the  $\text{O}_3$  mixing ratio with  $\text{HNO}_3$  held constant at  $40 (\pm 6)$  ppbv. The dependence of the normalised signal at  $m/z$  62 on  $[\text{O}_3]$  is clearly non-linear. We showed above that the sum of all  $\text{IO}_x^-$  anions increases approximately linearly with  $\text{O}_3$  mixing ratio while at the same time the behaviour of  $\text{IO}^-$  and  $\text{IO}_3^-$  is more complex. The sensitivity of  $\text{HNO}_3$  detection to changes in  $\text{O}_3$  concentration is expected to depend not only on the individual concentrations of each anion in the IMR but also on their respective rate coefficients for reaction with  $\text{HNO}_3$  (which are different, see above) and the observed non-linearity is not surprising. The solid lines through the data points are regressions of the form:

$$\text{Signal } (m/z \text{ 62}) = A(1 - \exp(-[\text{O}_3]B)) \quad (2)$$

Which reflects the expected, approximately exponential dependence of the concentration of  $\text{IO}_x^-$  in the IMR on the  $\text{O}_3$  concentration. In equation 2,  $[\text{O}_3]$  is the  $\text{O}_3$  mixing ratio in ppbv and  $B$  has a value of  $1.515 \times 10^{-3}$  per ppbv of  $\text{O}_3$ . As shown in Fig 7b, for a given  $[\text{HNO}_3]$ , the parameter  $A$  is dependent on the water vapour concentration (i.e. on ratio of signals at  $m/z$  145 and  $m/z$  127,  $(S_{145} / S_{127})$ ) over the range explored and can be parameterised as:

$$A = 0.138 + 0.929 \times (S_{145} / S_{127}) \quad (3)$$

In these experiments,  $\text{H}_2\text{O}$  was not added to the TD inlet (this would have increased the retention time of  $\text{HNO}_3$  on inlet surfaces, thereby making changes in the  $m/z$  62 difficult to interpret) but directly to the IMR, as described in section 2 and as used during airborne operation of the CIMS. The linear dependence of the signal at  $m/z$  62 on the ratio of signals at  $m/z$  145 and  $m/z$  127 at various ozone concentrations ( $[\text{HNO}_3]$  fixed at 38.5 ppbv) is further highlighted in Fig S3.

The positive intercept in Fig. 7b indicates that there is significant sensitivity to  $\text{HNO}_3$  detection at  $m/z$  62 in the absence of water in the IMR, implying that  $\text{IO}_x^-$  anions can react directly with  $\text{HNO}_3$  to form  $\text{NO}_3^-$  as written in R14-16. The increase in the sensitivity to  $\text{HNO}_3$  as the water vapour concentration is increased is consistent with the formation of  $\text{I}(\text{H}_2\text{O})$  ( $m/z$  145)

which reacts more rapidly with  $O_3$  (to form  $IO_2^-$  directly) than does  $I^-$  (Teiwes et al., 2019), thereby increasing the abundance of  $IO_X^-$  in the IMR (see above) and thus the instrument's sensitivity to  $HNO_3$ .

290 The very strong sensitizing effect of ozone and  $H_2O$  vapour can explain why similar instruments to ours observe large signals at  $m/z$  62 when sampling ambient air. Indeed, both  $O_3$  and  $HNO_3$  are ubiquitous and generally present at much higher levels than either  $NO_3$  or  $N_2O_5$ . Attempts to measure these trace gases using I-CIMS without TD-inlets and NO titration (to remove the  $HNO_3$  contribution) will likely result in erroneously high levels of both, especially during the day when lower-tropospheric  $O_3$  and  $HNO_3$  are often at their highest levels. It also explains why laboratory tests (generally carried out  
295 without added  $O_3$  or  $H_2O$ ) have shown only low (or no) sensitivity to  $HNO_3$  at  $m/z$  62.

### 3.2 Detection of $HNO_3$ at $m/z$ 190

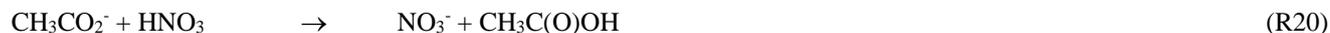
We now compare the detection of  $HNO_3$  at  $m/z$  62 to its detection at  $m/z$  190, the  $I(HNO_3)$  adduct, with various amounts of  $O_3$  present. In Fig. 8 we present the results of an experiment in which a constant flow of  $HNO_3$  (12.5 ppbv) was introduced into the inlet and the ozone mixing ratio was varied from zero to 900 ppbv. We observe a great increase in the signal at  $m/z$   
300 62 as expected (from 9 counts to > 6000 counts). At zero ozone, the signal at  $m/z$  190 is about 1000 counts and is largely background free, making this the preferred mass to monitor  $HNO_3$  in the absence of  $O_3$ . The cross-over point (when the signals at  $m/z$  62 and  $m/z$  190 are equal) is at an ozone mixing ratio of 100 ppbv. At an ozone mixing ratio of 800 ppbv, the signal at  $m/z$  62 is a factor 8.5 larger than that at  $m/z$  190.

Apparent from this figure is the depletion of the signal at  $m/z$  190 as the  $O_3$  mixing ratio increases to values of 800 ppbv, as  
305 present e.g. in the lower stratosphere. The solid lines are least-squares fits to the datasets that describe the exponential growth of the  $m/z$  62 signal as  $O_3$  is increased and the exponential decay of  $m/z$  190 over the same range. The reduction in signal at  $m/z$  190 is characterised by an exponential term  $\exp(-0.00046 \times [O_3])$  which means that at 800 ppbv  $O_3$  a ~30% reduction in sensitivity is observed. The loss of sensitivity at  $m/z$  190 is driven by the loss of  $I^-$  in the IMR as  $O_3$  is added. At the same time, the depletion of the signal at  $m/z$  127 is weaker, which reflects the fact that only a small fraction of  $IO_X^-$   
310 formed in the IMR are detected, the rest presumably being fragmented in the CDC before being detected as  $I^-$ .

The fact that some  $I^-$  is converted to  $IO_X^-$  in the IMR at high  $O_3$  levels but is not reflected in the  $I^-$  signal at  $m/z$  127 has repercussions for normalisation of product ion signals to the primary ion signal whereby the assumption is made that the measured signal at  $m/z$  127 stems only from  $I^-$ . In our instrument, the loss of  $I^-$  in the IMR is significant at high levels of  $O_3$  (e.g. 30 % at 800 ppbv  $O_3$ ). For this reason, we normalise the signals using values of the signal at  $m/z$  127 obtained by  
315 interpolating between measurements obtained when scrubbing the air. The normalisation problem may occur in other I-CIMS instruments to varying extents, and the degree of bias will depend on the conversion of  $I^-$  to  $IO_X^-$  and the extent to which  $IO_X^-$  is detected as  $I^-$ . The potential bias can be circumvented by the continuous addition of a calibration gas that is detected via reaction with  $I^-$ .

### 3.3 Detection of HNO<sub>3</sub> at *m/z* 62: The role of acetate anions

320 We have also evaluated the potential for “unintentional” HNO<sub>3</sub> detection at *m/z* 62 by its reaction with the acetate anion, CH<sub>3</sub>CO<sub>2</sub><sup>-</sup>:



The CH<sub>3</sub>CO<sub>2</sub><sup>-</sup> anion is the conjugate base of a weak acid (CH<sub>3</sub>C(O)OH) has been utilised to monitor a number of trace gases via proton transfer (Veres et al., 2008). While Veres et al. (2010) generated CH<sub>3</sub>CO<sub>2</sub><sup>-</sup> deliberately by passing acetic-  
325 anhydride through their <sup>210</sup>Po-source, in our experiments it is the product (monitored at *m/z* 59) of the reaction between I<sup>-</sup> primary ions and either CH<sub>3</sub>C(O)O<sub>2</sub> (from the thermal dissociation of PAN) or CH<sub>3</sub>C(O)OOH.



Figure 9a shows the result of a set of experiments demonstrating HNO<sub>3</sub> detection at *m/z* 62 without (blue data points) and  
330 with 3.25 ppbv of CH<sub>3</sub>C(O)OOH (black data points) added to the inlet flow. The initial (normalised) signal at *m/z* 59 from the CH<sub>3</sub>CO<sub>2</sub><sup>-</sup> anion in the absence of HNO<sub>3</sub> was 53500 counts. The presence of 3.25 ppbv CH<sub>3</sub>C(O)OOH (and resultant CH<sub>3</sub>CO<sub>2</sub><sup>-</sup>) results in a ~50-fold increase in the sensitivity of the I-CIMS to HNO<sub>3</sub>. We also carried out a few experiments (less systematic) in which PAN (instead of PAA) was added to the IMR and obtained the same results.

Our results disagree with the conclusions of Wang et al. (2014) who saw no increase at *m/z* 62 when adding PAN to air  
335 containing HNO<sub>3</sub> but are consistent with the use of CH<sub>3</sub>CO<sub>2</sub><sup>-</sup> as primary reactant ion to detect HNO<sub>3</sub> at *m/z* 62 (Veres et al., 2008). Figure 9b indicates that the increase in signal at *m/z* 62 when adding HNO<sub>3</sub> to a flow of CH<sub>3</sub>C(O)OOH in air is approximately proportional to the reduction in the ion-signal at *m/z* 59. This helps confirm that CH<sub>3</sub>CO<sub>2</sub><sup>-</sup> is the ion responsible for the detection of HNO<sub>3</sub> but also indicates that the detection of PAN and CH<sub>3</sub>C(O)OOH via conversion to CH<sub>3</sub>CO<sub>2</sub><sup>-</sup> can be compromised when HNO<sub>3</sub> is present in the air sample. Indeed, in many air masses the concentration of  
340 HNO<sub>3</sub> can be an order of magnitude greater than that of either PAN or CH<sub>3</sub>C(O)OOH and given that other abundant trace gases (e.g. organic acids) also react with CH<sub>3</sub>CO<sub>2</sub><sup>-</sup> (Veres et al., 2008) further reactions of CH<sub>3</sub>CO<sub>2</sub><sup>-</sup> in the ion-molecule reactor regions of I-CIMS instruments may result in a significant bias (to lower values) which would have to be analysed case-by-case for different instruments. **One way to avoid this problem is the continuous addition of isotopically labelled PAN to the inlet (see e.g. Roiger et al. (2011)) as the secondary, reactive losses of <sup>12</sup>C and <sup>13</sup>C CH<sub>3</sub>CO<sub>2</sub><sup>-</sup> are expected to be**  
345 **identical.**

Wang et al. (2014) observed that the majority of the *m/z* 62 signal during the daytime could be removed by addition of NO  
(0.54 ppmv or 1.3 × 10<sup>13</sup> molecule cm<sup>-3</sup>) to the inlet. At their inlet temperature of 120-180 °C, NO reacts with O<sub>3</sub> with a rate coefficient in the range 6-9 × 10<sup>-14</sup> cm<sup>3</sup> molecule<sup>-1</sup> s<sup>-1</sup>, which results in a half-life for O<sub>3</sub> of 500 to 800 ms. Wang et al. (2014) do not mention the residence time of air passing through their heated inlet, but it appears plausible that a substantial fraction  
350 of ambient O<sub>3</sub> would have been removed during background measurement, thus decreasing (or removing) sensitivity towards

HNO<sub>3</sub> via reactions involving O<sub>3</sub> in the IMR, and leading the authors to conclude that NO<sub>3</sub> was being detected above a lower background than truly present.

To illustrate the potential size of the bias due to HNO<sub>3</sub> when monitoring N<sub>2</sub>O<sub>5</sub> at  $m/z$  62 in field measurements we take the relative sensitivities (at  $m/z$  62) of our I-CIMS to N<sub>2</sub>O<sub>5</sub> and to HNO<sub>3</sub> (in the presence of typical boundary layer mixing ratios of O<sub>3</sub> (50 ppbv) and at typical relative humidity (50%). Under these conditions, with N<sub>2</sub>O<sub>5</sub> and HNO<sub>3</sub> mixing ratios of 0.2 and 2 ppbv, respectively, we calculate that HNO<sub>3</sub> would account for > 70% of the signal at  $m/z$  62.

## 4 Field Measurements

Having shown that HNO<sub>3</sub> is detected by our I-CIMS with reasonable sensitivity when sufficient O<sub>3</sub> is present in ambient air samples, we now examine the signals at  $m/z$  62 obtained in airborne operation of the I-CIMS during two CAFE (Chemistry of the Atmosphere Field Experiment) campaigns of the HALO aircraft. In the CAFE-Africa campaign (2018) the I-CIMS monitored  $m/z$  62 on several flights over the Atlantic west of the African continent. During the 2020 CAFE-EU campaign with HALO over Europe, the I-CIMS additionally monitored  $m/z$  190 (the I(HNO<sub>3</sub>) cluster ion) which is selective to HNO<sub>3</sub>. During both campaigns, O<sub>3</sub> and H<sub>2</sub>O (required for analysis of the signal at  $m/z$  62) were routinely measured.

### 4.1 CAFÉ-Africa

Here we examine the results obtained during a HALO flight as part of the CAFE-Africa mission. The flight in question was the transfer from Sal airport on the Cape Verde islands (which served as base-station during the mission) back to Germany. During the flight the aircraft flew mainly at high altitudes (13-15 km) so that stratospheric air was sampled at higher latitudes but also made two dives into the free-troposphere. The flight track is displayed in Fig S4.

Figure 10 shows a time-series of ozone mixing ratios during the flight (panel a) along with the I-CIMS signal at  $m/z$  62 (panel b). In air masses with stratospheric influence (i.e. O<sub>3</sub> values > 100 ppb, 12:20 -15:10 UTC) there is an obvious, strong co-variance between these two parameters. However, once corrected for the dependence of the sensitivity of the I-CIMS to O<sub>3</sub> (equations 2 and 3) we obtain the black line representing the mixing ratios of HNO<sub>3</sub> and the covariance is greatly reduced. We also note that, apart from some significant increases at ~11:30 and ~16:00 the HNO<sub>3</sub> mixing ratio decreases slowly throughout the flight, which is the result of HNO<sub>3</sub> generation in the <sup>210</sup>Po source leading to an initially large background signal. The formation of HNO<sub>3</sub> in the <sup>210</sup>Po source has been documented previously (Ji et al., 2020); its level can be reduced by permanently flushing N<sub>2</sub> through the source while keeping the mass-spectrometer under operational vacuum. This was not carried out during the CAFE missions on HALO as continuous operation of the instrument (i.e. overnight between flights) was not possible. We note that the background signal at  $m/z$  62 that originates from the polonium source cannot be obtained by scrubbing the air of HNO<sub>3</sub> as this also removes O<sub>3</sub> and thus also sensitivity to HNO<sub>3</sub> at this mass.

380 A roughly exponential decay of the HNO<sub>3</sub> background signal was observed in all of the flights in which *m/z* 62 was monitored, which presumably reflects depletion of the initially large HNO<sub>3</sub> reservoir which was built up when the I-CIMS was switched off.

A coarse correction of the dataset was thus undertaken by subtracting an exponentially decaying background from the total HNO<sub>3</sub> signal. The resulting HNO<sub>3</sub> mixing ratios are depicted as the blue line in Fig. 10b and plotted against the O<sub>3</sub> mixing ratio in Fig. 10c. Considering only the high altitude data for which O<sub>3</sub> mixing ratios were > 100 ppbv (stratospheric influence, black data points) we derive a slope of HNO<sub>3</sub> / O<sub>3</sub> =  $(3 \pm 0.5) \times 10^{-3}$  (the uncertainty is 2  $\sigma$ , statistical only) which is consistent with previously reported values obtained in airborne measurements of HNO<sub>3</sub> and O<sub>3</sub> in the lower stratosphere (see Popp et al. (2009) and references therein). We stress that deriving accurate mixing ratios of HNO<sub>3</sub> is not possible with this data set and the values obtained are strongly dependent on the background correction. Here, we merely wish to indicate that, while most of the variability in our *m/z* 62 signal is related to the central role of ozone in the detection scheme (i.e. formation of IO<sub>x</sub>), some covariance between HNO<sub>3</sub> and O<sub>3</sub> remains after correction of the raw data and the slope is roughly in line with that expected. We also do not propose that the correlation of *m/z* 62 with O<sub>3</sub> proves that the signal can be attributed entirely to HNO<sub>3</sub>. This aspect will be covered in section 4.2.

Figure 10b reveals sharp increases in the (background corrected) HNO<sub>3</sub> mixing ratio when sampling at lower altitudes, noticeably at 11:30- 12:00 (3.9 km altitude) and at 15:45-16:10 (4.7 km altitude) and at the end of the flight during descent to Oberpfaffenhofen in Bavaria, Germany. In all cases, these periods of enhanced HNO<sub>3</sub> coincided with higher levels of particles. Back trajectories (HYSPLIT) indicated that, in the 10 days prior to interception by HALO, the air mass sampled at 11:30 had passed over the West African continent (Mauritania, Mali and Niger), whereas the air masses sampled after 16:00 were of European origin. The large, coincidental increase in the HNO<sub>3</sub> mixing ratio and particle mass was a recurrent feature of the CAFE-Africa flights. It is conceivable that the HNO<sub>3</sub> measured by the I-CIMS was a mixture of gas-phase HNO<sub>3</sub> and HNO<sub>3</sub> associated with particles that desorb HNO<sub>3</sub> when passing through the thermal dissociation inlet at 180 °C. This temperature would be sufficient to thermally convert ammonium nitrate to HNO<sub>3</sub> (and NH<sub>3</sub>) as well as to result in the desorption of HNO<sub>3</sub> that was physi-sorbed e.g. on chemically aged black-carbon or mineral-dust particles. As we do not know the efficiency with which particles of various diameters enter the TD-inlet of the CIMS, we cannot estimate the relative contribution of gas-phase and particulate nitrate to the signal at *m/z* 62 but indicate that a similar phenomenon may occur in ground-based measurements using TD-inlets and may represent an additional source of bias during ambient measurements of NO<sub>3</sub> and/or N<sub>2</sub>O<sub>5</sub> at *m/z* 62.

## 4.2 CAFE-Europa

During the CAFE-Europe HALO flights the I-CIMS monitored *m/z* 190, the I(HNO<sub>3</sub>) adduct, as well as NO<sub>3</sub><sup>-</sup> at *m/z* 62. The detection of HNO<sub>3</sub> at *m/z* 190 varies with the water vapour concentration in the IMR: The response of the HNO<sub>3</sub> signal at *m/z* 190 to changes in the HNO<sub>3</sub> concentration and in the *m/z* 145 / *m/z* 127 ratio (i.e. the relative humidity in the IMR, see Fig. S2) is illustrated in Fig. S5.

Figure 11 displays a set of data obtained during a flight on the 30th May 2020 on which the HALO aircraft flew a path from Southern Germany to the Atlantic (west of Ireland) and back at various altitudes (for flight track see Fig S6). Figure 11a plots the raw signals measured by the I-CIMS at  $m/z$  62 and  $m/z$  190 as well as the  $O_3$  mixing ratio. **Similar to the CAFE-Africa dataset, the signal at  $m/z$  62 covaries strongly with the  $O_3$  mixing ratios, which were between  $\sim 40$  and  $\sim 700$  ppbv whereas the raw signals at  $m/z$  62 and  $m/z$  190 (both due to  $HNO_3$ ) bear little resemblance to each other.**

Using the **calibration** parameters described in section 3 and (for  $m/z$  190) in Fig. S3, the signals at  $m/z$  62 and  $m/z$  190 were converted to  $HNO_3$  mixing ratios, depicted in Fig. 11b. Despite the greatly divergent raw-signals, the  $HNO_3$  mixing ratios obtained using the different mass-to-charge ratios are in reasonable agreement, both displaying a gradual decrease after take-off at  $\sim 08:00$  UTC. The high initial level of  $HNO_3$  is largely the result of  $HNO_3$  being formed in the  $^{210}Po$  source during overnight instrument shut-down (see section 4.1). The  $HNO_3$  mixing ratios observed at  $m/z$  62 and  $m/z$  190 both increase when the aircraft sampled stratospheric air (11:00 to 13:00 and 15:10-15:30 UTC). In Fig. 11c  $HNO_3$  mixing ratios derived at  $m/z$  62 and  $m/z$  190 are plotted in a correlation diagram. **The slope ( $1.14 \pm 0.05$ ) and intercept ( $-0.3 \pm 0.3$ ) indicate reasonable agreement even when the raw signals are greatly divergent at high levels of  $O_3$ . At the highest levels of  $O_3$ , some differences in the retrieved mixing ratios of  $HNO_3$  using  $m/z$  62 and  $m/z$  190 are observed, which, given the large,  $O_3$ -dependent corrections applied (especially for  $m/z$  62) is not surprising. Our airborne data show that in many (if not most) air masses,  $m/z$  62 provides a measure of  $HNO_3$  rather than  $NO_3$  and  $N_2O_5$ .**

## 5 Conclusions

A series of laboratory experiments investigating the origin of signal at  $m/z$  62 when using an I-CIMS has revealed unexpected sensitivity to  $HNO_3$  at this mass-to-charge ratio in the presence of  $O_3$  or peroxyacetic acid (PAA) or PAN. The ozone effect is related to the formation of  $IO_x^-$  which react rapidly with  $HNO_3$  to form  $NO_3^-$  thus bypassing the thermodynamic barrier to formation of  $NO_3^-$  by direct reaction of  $HNO_3$  with  $I^-$ . The presence of  $O_3$  at a mixing ratio of 500 ppbv results in a 250-fold increase in sensitivity to  $HNO_3$  at  $m/z$  62. The sensitivity to  $HNO_3$  at this mass-to-charge ratio was also found to be highly dependent on the concentration of  $H_2O$  in the ion-molecule reactor as this aids formation of  $IO_x^-$ . The sensitivity to  $HNO_3$  at  $m/z$  62 in the presence of PAA is a result of the presence of acetate anions ( $CH_3CO_2^-$ ) as demonstrated previously (Veres et al., 2008). **We conclude that measurements of PAN using I-CIMS may be biased to low values if large mixing ratios of  $HNO_3$  (or organic acids) are present and continuous calibration (e.g. with isotopically labelled PAN) is not carried out.** Our laboratory experiments indicate that measurements of atmospheric  $NO_3$  and  $N_2O_5$  at  $m/z$  62 can be heavily biased by the presence of  $HNO_3$ , and may explain reports of unexpectedly high daytime mixing ratios of  $N_2O_5$ . The relative sensitivity at  $m/z$  62 to  $HNO_3$  and  $N_2O_5 / NO_3$  will vary from one I-CIMS instrument to the next and must thus be analysed case-by-case.

We have examined signals at  $m/z$  62 during two periods of operation of the I-CIMS on the HALO-aircraft, one over the Atlantic west of the African coast and one over Europe. During the flights over Europe  $HNO_3$  mixing ratios derived from  $m/z$

445 62 NO<sub>3</sub><sup>-</sup> and at *m/z* 190 (I<sup>-</sup>(HNO<sub>3</sub>)) were in good agreement. The data obtained over the Atlantic indicated that measurements at *m/z* 62 using a thermal dissociation inlet can be strongly influenced by particulate nitrate that can thermally dissociate (or desorb) to gas-phase HNO<sub>3</sub>.

### Data availability

450 Data measured during the flight campaign CAFE campaigns are available to all scientists agreeing to the CAFE data protocol. The laboratory data underlying the Figures is available upon request to the authors.

### Author contributions

RD conducted the laboratory experiments, carried out the airborne measurements with assistance from PE and JC and analysed the laboratory data with assistance from JC. The manuscript was written by JC and RD with contributions from all other authors. JL designed and helped plan the airborne operations.

### 455 Competing interests

The authors declare that they have no conflict of interest.

### Acknowledgments

460 We acknowledge the collaboration with the DLR (German Aerospace Centre) during the HALO campaigns CAFE- Africa and CAFE-EU. We thank Florian Obersteiner and Andreas Zahn (KIT-Karlsruhe) for use of the O<sub>3</sub>-data during CAFE-Africa and CAFE-EU.

### References

465 Atkinson, R., Baulch, D. L., Cox, R. A., Crowley, J. N., Hampson, R. F., Hynes, R. G., Jenkin, M. E., Rossi, M. J., and Troe, J.: Evaluated kinetic and photochemical data for atmospheric chemistry: Volume I - gas phase reactions of Ox, HOx, NOx and SOx species, *Atmos. Chem. Phys.*, 4, 1461-1738, doi:10.5194/acp-4-1461-2004, 2004.

Bhujel, M., Marshall, D. L., Maccarone, A. T., McKinnon, B. I., Trevitt, A. J., da Silva, G., Blanksby, S. J., and Poad, B. L. J.: Gas phase reactions of iodide and bromide anions with ozone: evidence for stepwise and reversible reactions, *Phys. Chem. Chem. Phys.*, 22, 9982-9989, doi:10.1039/d0cp01498b, 2020.

470 Chang, W. L., Bhave, P. V., Brown, S. S., Riemer, N., Stutz, J., and Dabdub, D.: Heterogeneous atmospheric chemistry, ambient measurements and model calculations of N<sub>2</sub>O<sub>5</sub>: A review, *Aerosol. Sci. Tech.*, 45, 655-685, doi:10.1080/02786826.2010.551672, 2011.

475 Crowley, J. N., Ammann, M., Cox, R. A., Hynes, R. G., Jenkin, M. E., Mellouki, A. M., Rossi, M. J., Troe, J., and Wallington, T. J.: Evaluated kinetic and photochemical data for atmospheric chemistry: Volume V - heterogeneous reactions on solid substrates, *Atmos. Chem. Phys.*, 10, 9059-9223, 2010.

- Davidson, J. A., Viggiano, A. A., Howard, C. J., Dotan, I., Fehsenfeld, F. C., Albritton, D. L., and Ferguson, E. E.: Rate Constants for Reactions of  $O_2^+$ ,  $NO_2^+$ ,  $NO^+$ ,  $H_3O^+$ ,  $CO_3^-$ ,  $NO_2^-$ , and Halide Ions with  $N_2O_5$  at 300 K, *J. Chem. Phys.*, 68, 2085-2087, 1978.
- 480 Dubé, W. P., Brown, S. S., Osthoff, H. D., Nunley, M. R., Ciciora, S. J., Paris, M. W., McLaughlin, R. J., and Ravishankara, A. R.: Aircraft instrument for simultaneous, in situ measurement of  $NO_3$  and  $N_2O_5$  via pulsed cavity ring-down spectroscopy, *Rev. Sci. Instrum.*, 77, doi: 10.1063/1.2176058, 2006.
- Dulitz, K., Amedro, D., Dillon, T. J., Pozzer, A., and Crowley, J. N.: Temperature-(208-318 K) and pressure-(18-696 Torr) dependent rate coefficients for the reaction between OH and  $HNO_3$ , *Atmos. Chem. Phys.*, 18, 2381-2394, 2018.
- 485 Eger, P. G., Helleis, F., Schuster, G., Phillips, G. J., Lelieveld, J., and Crowley, J. N.: Chemical ionization quadrupole mass spectrometer with an electrical discharge ion source for atmospheric trace gas measurement, *Atmos. Meas. Tech.*, 12, 1935-1954, doi:10.5194/amt-12-1935-2019, 2019.
- Fehsenfeld, F. C., Howard, C. J., and Schmeltekopf, A. L.: Gas phase ion chemistry of  $HNO_3$ , *The Journal of Chemical Physics*, 63, 2835-2841, doi:10.1063/1.431722, 1975.
- 490 Fischer, H., Waibel, A. E., Welling, M., Wienhold, F. G., Zenker, T., Crutzen, P. J., Arnold, F., Burger, V., Schneider, J., Bregman, A., Lelieveld, J., and Siegmund, P. C.: Observations of high concentrations of total reactive nitrogen (NOy) and nitric acid ( $HNO_3$ ) in the lower Arctic stratosphere during the stratosphere-troposphere experiment by aircraft measurements (STREAM) II campaign in February 1995, *J. Geophys. Res. -Atmos.*, 102, 23559-23571, doi:10.1029/97jd02012, 1997.
- Goos, E., Burcat, A., and Ruscic, B.: Extended Third Millennium Ideal Gas and Condensed Phase Thermochemical Database for Combustion with Updates from Active Thermochemical Tables: Update of "Third Millennium Ideal Gas and Condensed Phase Thermochemical Database for Combustion with Updates from Active Thermochemical Tables by Alexander Burcat and Branko Ruscic", Report ANL 05/20 and TAE 960 Technion-IIT, Aerospace Engineering, and Argonne National Laboratory, Chemistry Division, September 2005., 2005.
- 495 Hanson, D. R., and Ravishankara, A. R.: The reaction probabilities of  $ClONO_2$  and  $N_2O_5$  on polar stratospheric cloud material, *JGR*, 96, 5081-5090, 1991.
- 500 Huey, L. G., Hanson, D. R., and Howard, C. J.: Reactions of  $SF_6^-$  and  $I^-$  with atmospheric trace gases, *J. Phys. Chem.*, 99, 5001-5008, doi:10.1021/j100014a021, 1995.
- Huey, L. G.: The kinetics of the reactions of  $Cl^-$ ,  $O^-$ , and  $O_2^-$  with  $HNO_3$ : Implications for measurement of  $HNO_3$  in the atmosphere, *Int. J. Mass Spectrom. Ion Processes*, 153, 145-150, doi:10.1016/0168-1176(95)04354-3, 1996.
- 505 Huey, L. G.: Measurement of trace atmospheric species by chemical ionization mass spectrometry: Speciation of reactive nitrogen and future directions, *Mass Spectrom. Rev.*, 26, 166-184, doi:10.1002/mas.20118, 2007.
- Task Group on Atmospheric Chemical Kinetic Data Evaluation, (Ammann, M., Cox, R.A., Crowley, J.N., Herrmann, H., Jenkin, M.E., McNeill, V.F., Mellouki, A., Rossi, M. J., Troe, J. and Wallington, T. J.): <http://iupac.pole-ether.fr/index.html>, 2021.
- 510 Iyer, S., He, X. C., Hyttinen, N., Kurten, T., and Rissanen, M. P.: Computational and experimental investigation of the detection of  $HO_2$  radical and the products of its reaction with cyclohexene ozonolysis derived  $RO_2$  radicals by an iodide-based chemical ionization mass spectrometer, *J. Phys. Chem. A*, 121, 6778-6789, doi:10.1021/acs.jpca.7b01588, 2017.
- Ji, Y., Huey, L. G., Tanner, D. J., Lee, Y. R., Veres, P. R., Neuman, J. A., Wang, Y., and Wang, X.: A vacuum ultraviolet ion source (VUV-IS) for iodide-chemical ionization mass spectrometry: a substitute for radioactive ion sources, *Atmos. Meas. Tech.*, 13, 3683-3696, doi:10.5194/amt-13-3683-2020, 2020.
- 515 Kercher, J. P., Riedel, T. P., and Thornton, J. A.: Chlorine activation by  $N_2O_5$ : simultaneous, in situ detection of  $ClONO_2$  and  $N_2O_5$  by chemical ionization mass spectrometry, *Atmos. Meas. Tech.*, 2, 193-204, doi:10.5194/amt-2-193-2009, 2009.
- Khanniche, S., Louis, F., Cantrel, L., and Černušák, I.: A theoretical study of the microhydration of iodic acid ( $HOIO_2$ ), *Computational and Theoretical Chemistry*, 1094, 98-107, doi:<https://doi.org/10.1016/j.comptc.2016.09.010>, 2016.

- 520 Lee, B. H., Lopez-Hilfiker, F. D., Mohr, C., Kurten, T., Worsnop, D. R., and Thornton, J. A.: An iodide-adduct high-resolution time-of-flight chemical-ionization mass spectrometer: Application to atmospheric inorganic and organic compounds, *Env. Sci. Tech.*, 48, 6309-6317, doi:10.1021/es500362a, 2014.
- Lengyel, J., Oncak, M., and Beyer, M. K.: Chemistry of NO<sub>x</sub> and HNO<sub>3</sub> molecules with gas-phase hydrated O<sup>-</sup> and OH<sup>-</sup> ions, *Chemistry-a European Journal*, 26, 7861-7868, doi:10.1002/chem.202000322, 2020.
- 525 Lightfoot, P. D., Cox, R. A., Crowley, J. N., Destriau, M., Hayman, G. D., Jenkin, M. E., Moortgat, G. K., and Zabel, F.: Organic peroxy radicals - kinetics, spectroscopy and tropospheric chemistry, *Atmos. Environ., Part A*, 26, 1805-1961, 1992.
- McCracken, F. L.: Total collision cross sections of negative atomic iodine ions in nitrogen and argon, 1952.
- 530 Phillips, G. J., Pouvesle, N., Thieser, J., Schuster, G., Axinte, R., Fischer, H., Williams, J., Lelieveld, J., and Crowley, J. N.: Peroxyacetyl nitrate (PAN) and peroxyacetic acid (PAA) measurements by iodide chemical ionisation mass spectrometry: first analysis of results in the boreal forest and implications for the measurement of PAN fluxes, *Atmos. Chem. Phys.*, 13, 1129-1139, doi:doi:10.5194/acp-13-1129-2013, 2013.
- Popp, P. J., Marcy, T. P., Gao, R. S., Watts, L. A., Fahey, D. W., Richard, E. C., Oltmans, S. J., Santee, M. L., Livesey, N. J., Froidevaux, L., Sen, B., Toon, G. C., Walker, K. A., Boone, C. D., and Bernath, P. F.: Stratospheric correlation between nitric acid and ozone, *J. Geophys. Res. -Atmos.*, 114, 10, doi:10.1029/2008jd010875, 2009.
- 535 Riva, M., Rantala, P., Krechmer, J. E., Peräkylä, O., Zhang, Y., Heikkinen, L., Garmash, O., Yan, C., Kulmala, M., Worsnop, D., and Ehn, M.: Evaluating the performance of five different chemical ionization techniques for detecting gaseous oxygenated organic species, *Atmos. Meas. Tech.*, 12, 2403-2421, doi:10.5194/amt-12-2403-2019, 2019.
- Roiger, A., Aufmhoff, H., Stock, P., Arnold, F., and Schlager, H.: An aircraft-borne chemical ionization - ion trap mass spectrometer (CI-ITMS) for fast PAN and PPN measurements, *Atmos. Meas. Tech.*, 4, 173-188, doi:doi:10.5194/amt-4-173-2011, 2011.
- 540 Slusher, D. L., Huey, L. G., Tanner, D. J., Flocke, F. M., and Roberts, J. M.: A thermal dissociation-chemical ionization mass spectrometry (TD-CIMS) technique for the simultaneous measurement of peroxyacyl nitrates and dinitrogen pentoxide, *J. Geophys. Res. -Atmos.*, 109, Art Nr. D19315, doi:10.1029/2004JD004670, 2004.
- 545 Teiwes, R., Elm, J., Handrup, K., Jensen, E. P., Bilde, M., and Pedersen, H. B.: Atmospheric chemistry of iodine anions: elementary reactions of I<sup>-</sup>, IO<sup>-</sup>, and IO<sub>2</sub><sup>-</sup> with ozone studied in the gas-phase at 300 K using an ion trap, *Phys. Chem. Chem. Phys.*, 20, 28606-28615, doi:10.1039/c8cp05721d, 2018.
- Teiwes, R., Elm, J., Bilde, M., and Pedersen, H. B.: The reaction of hydrated iodide I(H<sub>2</sub>O)<sup>-</sup> with ozone: a new route to IO<sub>2</sub><sup>-</sup> products, *Phys. Chem. Chem. Phys.*, 21, 17546-17554, doi:10.1039/c9cp01734h, 2019.
- 550 Veres, P., Roberts, J. M., Warneke, C., Welsh-Bon, D., Zahniser, M., Herndon, S., Fall, R., and de Gouw, J.: Development of negative-ion proton-transfer chemical-ionization mass spectrometry (NI-PT-CIMS) for the measurement of gas-phase organic acids in the atmosphere, *Int. J. Mass Spectrom.*, 274, 48-55, doi:10.1016/j.ijms.2008.04.032, 2008.
- Veres, P., Gilman, J. B., Roberts, J. M., Kuster, W. C., Warneke, C., Burling, I. R., and de Gouw, J.: Development and validation of a portable gas phase standard generation and calibration system for volatile organic compounds, *Atmos. Meas. Tech.*, 3, 683-691, doi:pil, 2010.
- 555 Wang, X., Wang, T., Yan, C., Tham, Y. J., Xue, L., Xu, Z., and Zha, Q.: Large daytime signals of N<sub>2</sub>O<sub>5</sub> and NO<sub>3</sub> inferred at 62 amu in a TD-CIMS: chemical interference or a real atmospheric phenomenon?, *Atmos. Meas. Tech.*, 7, 1-12, doi:10.5194/amt-7-1-2014, 2014.
- Wayne, R. P., Barnes, I., Biggs, P., Burrows, J. P., Canosa-Mas, C. E., Hjorth, J., Le Bras, G., Moortgat, G. K., Perner, D., Poulet, G., Restelli, G., and Sidebottom, H.: The nitrate radical: Physics, chemistry, and the atmosphere, *Atmos. Env. A*, 25A, 1-206, 1991.
- 560 Williams, S., Campos, M. F., Midey, A. J., Arnold, S. T., Morris, R. A., and Viggiano, A. A.: Negative ion chemistry of ozone in the gas phase, *J. Phys. Chem. A*, 106, 997-1003, doi:10.1021/jp012929r, 2002.

Wincel, H., Mereand, E., and Castleman, A. W.: Gas phase reactions of  $\text{DNO}_3$  with  $\text{X}^-(\text{D}_2\text{O})_n$ ,  $\text{X}=\text{O}$ ,  $\text{OD}$ ,  $\text{O}_2$ ,  $\text{DO}_2$ , and  $\text{O}_3$ , *J. Phys. Chem.*, 100, 7488-7493, doi:10.1021/jp953104i, 1996.

565

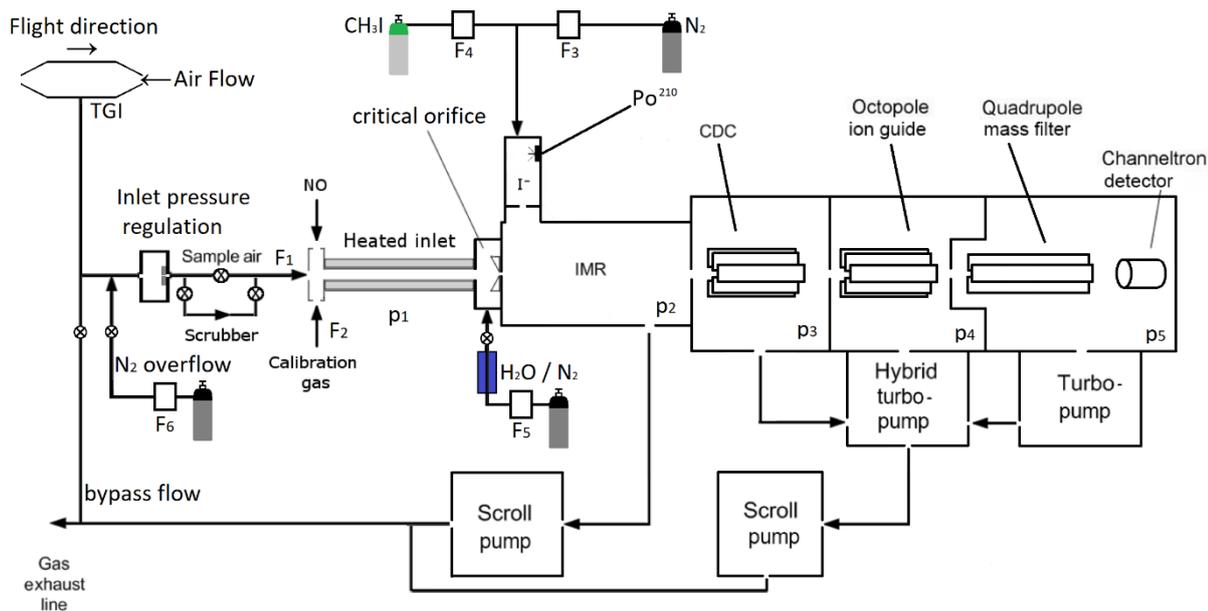
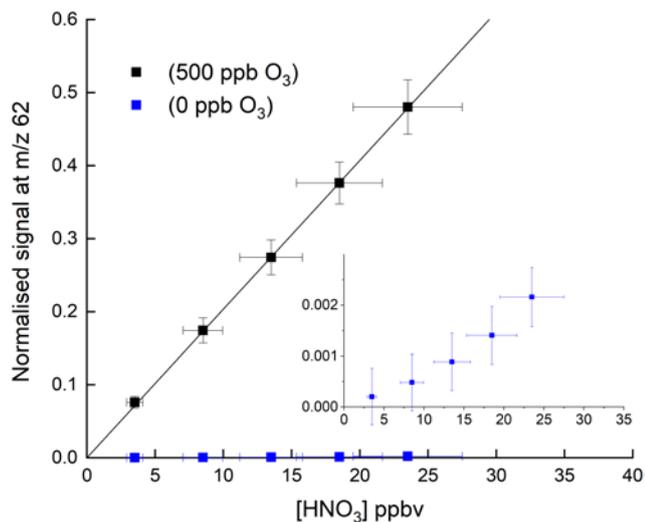


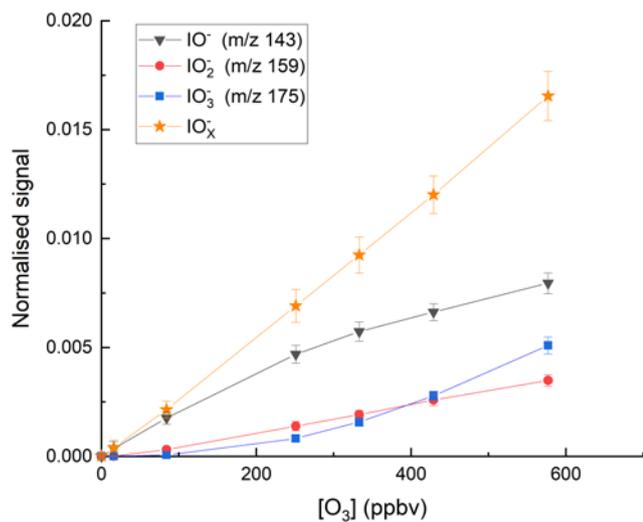
**Figure 1** Schematic diagram illustrating the central components of the I-CIMS used in this work. IMR = ion-molecule reactor, CDC = collisional dissociation chamber,  $F_1 = 1250 \text{ cm}^3 \text{ (STP) min}^{-1}$ ,  $F_2 = 50 \text{ cm}^3 \text{ (STP) min}^{-1}$ ,  $F_3 = 750 \text{ cm}^3 \text{ (STP) min}^{-1}$ ,  $F_4 = 4 \text{ cm}^3 \text{ (STP) min}^{-1}$ ,  $F_5 = 50 \text{ cm}^3 \text{ (STP) min}^{-1}$ .  $p_1 = 100 \text{ mbar}$ ,  $p_2 = 24 \text{ mbar}$ ,  $p_3 = 0.6 \text{ mbar}$ ,  $p_4 = 6 \times 10^{-3} \text{ mbar}$ ,  $p_5 = 9 \times 10^{-5} \text{ mbar}$ . The heated inlet is made of PFA-tubing. TGI = Trace-gas-inlet. **When overflowing the inlet line, the valve to the exhaust line is closed. When sampling air, the valve to the  $\text{N}_2$  bottle is closed.**

575



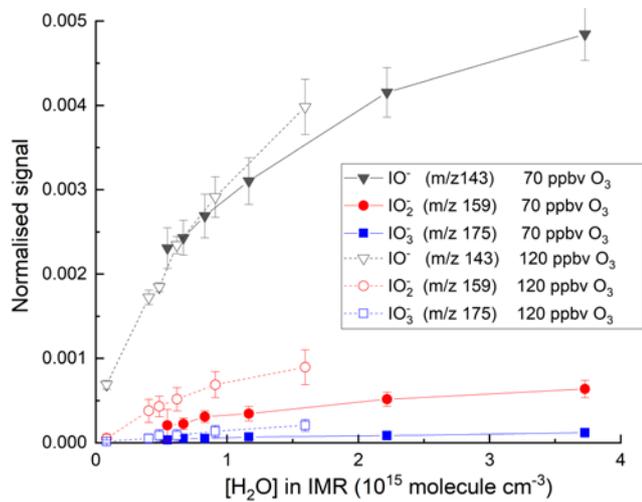
580 **Figure 2.** HNO<sub>3</sub> detection at  $m/z$  62 in the absence and presence (500 ppbv) of O<sub>3</sub>. The solid lines are non-weighted, linear regressions to the data and are  $2.035 \times 10^{-2}$  and  $8.033 \times 10^{-5}$  ppbv<sup>-1</sup> HNO<sub>3</sub> when 500 ppbv O<sub>3</sub> or zero O<sub>3</sub> were present, respectively. The inset (same x- and y-axes as in the full figure) is an expanded view of the signal obtained in the absence of O<sub>3</sub>. The error bars represent 15% systematic uncertainty in the HNO<sub>3</sub> concentration and  $2\sigma$  statistical uncertainty in the signal at  $m/z$  62.

585



590

**Figure 3:** Variation of the I-CIMS signals at  $m/z$  143 ( $\text{IO}^-$ ), 159 ( $\text{IO}_2^-$ ) and 175 ( $\text{IO}_3^-$ ) with the mixing ratios of  $\text{O}_3$ . The  $\text{O}_3$  mixing ratios are those measured in air before the gas-flow entered the inlet. The water vapour was held constant using our standard setting ( $[\text{H}_2\text{O}]_{\text{IMR}} = 2.9 \times 10^{14} \text{ molecule cm}^{-3}$ ).



595

**Figure 4:** Variation in the total ion signal (counts) due to IO<sup>-</sup>, IO<sub>2</sub><sup>-</sup> and IO<sub>3</sub><sup>-</sup> with the concentration of water vapour in the IMR. The results are from two sets of experiments where the O<sub>3</sub> mixing ratio was either 70 or 120 ppbv.

600

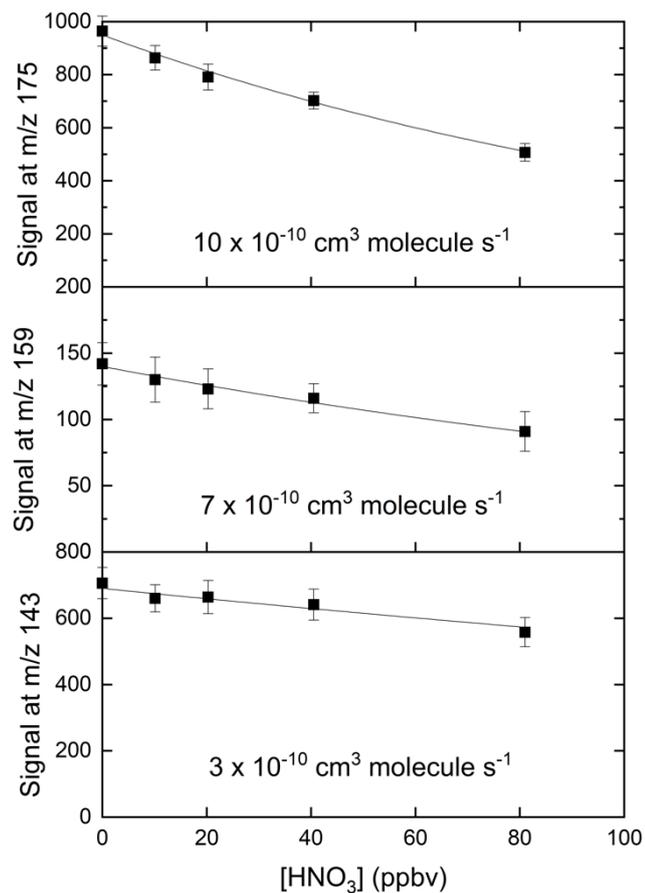


**Figure 5:** Relative changes in signals at  $m/z$  143 ( $\text{IO}^-$ ),  $m/z$  159 ( $\text{IO}_2^-$ ) and  $m/z$  175 ( $\text{IO}_3^-$ ) when adding up to 80 ppbv of  $\text{HNO}_3$ . The rate coefficients were calculated using a reaction time of 25 ms and should thus only be regarded as approximate.

605

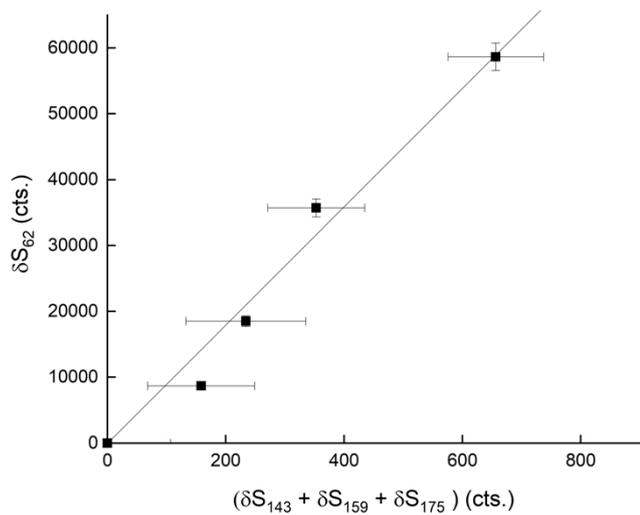
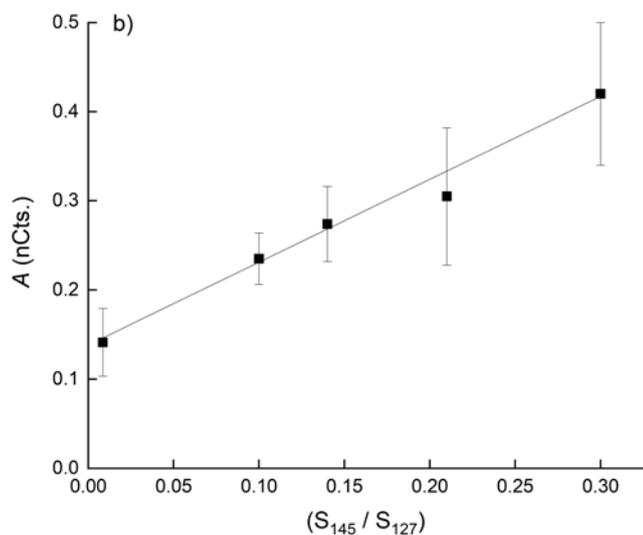
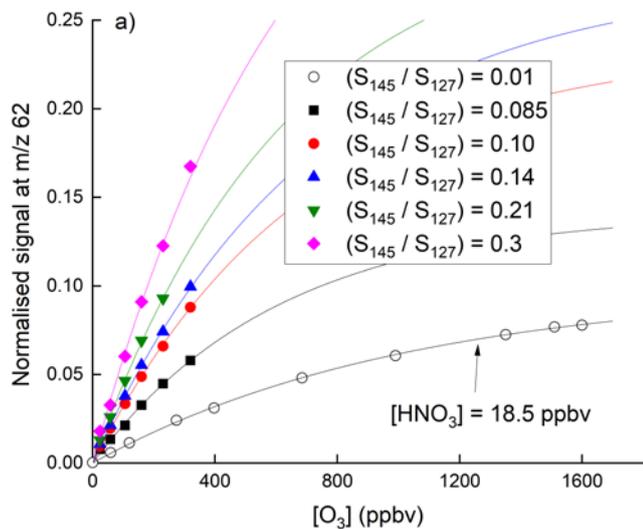


**Figure 6:** Relative changes in the sum of signals at  $m/z$  143 ( $\text{IO}^-$ ),  $m/z$  159 ( $\text{IO}_2^-$ ) and  $m/z$  175 ( $\text{IO}_3^-$ ) when adding up to 80 ppbv of  $\text{HNO}_3$ .  $\delta$  refers to the change in signal upon adding  $\text{HNO}_3$  and thus takes background signals at each mass-to-charge ratio into account.



615 **Figure 7.** a) Dependence of the signal at  $m/z$  62 on the  $O_3$  mixing ratio for 6 different concentrations of  $H_2O$  in the IMR. In the upper 5 curves (solid symbols) the  $HNO_3$  mixing ratio was 38.5 ppbv. In the lowermost curve, the  $HNO_3$  mixing ratio was 18.5 ppbv, as indicated. The fits lines are of the form:  $y = A \cdot \exp(1 - \exp(-B \cdot [O_3]))$ . b) Plot of parameter  $A$  versus the relative signal at  $m/z$  145 and  $m/z$  127.

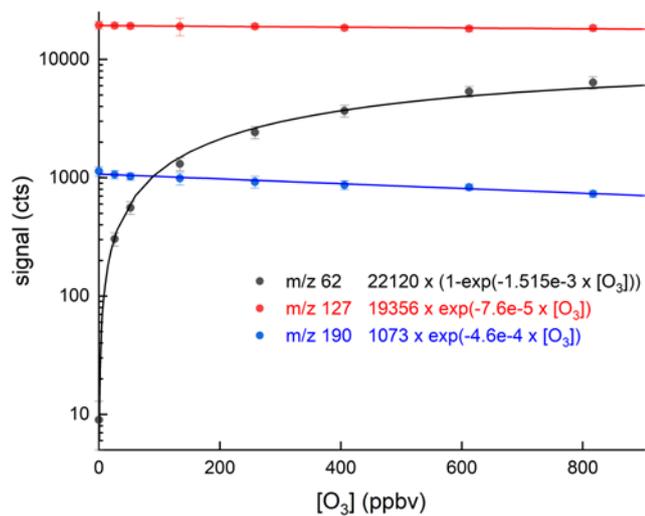
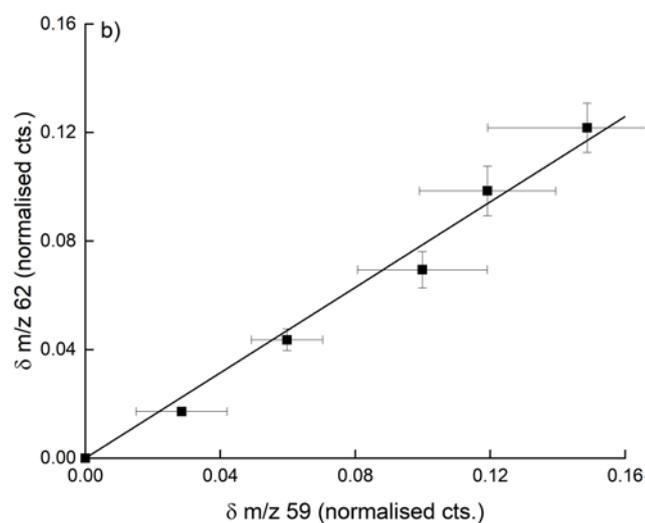
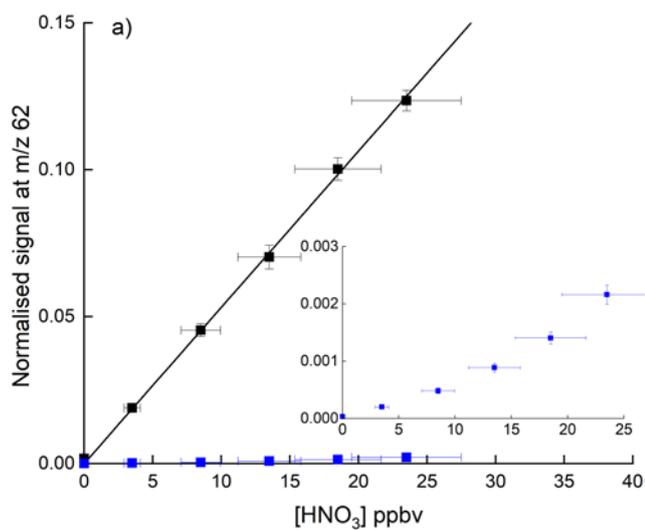


**Figure 8.** Dependence of the signals at  $m/z$  62 and  $m/z$  190 on the  $O_3$  mixing ratio with  $HNO_3$  fixed at 12.5 ppbv. The lines through the data are described by the expressions listed in the Figure.



630 **Figure 9.** a) Detection of  $\text{HNO}_3$  at  $m/z$  62 in the presence of 3.25 ppbv PAA (and thus the acetate anion,  $\text{CH}_3\text{CO}_2$ ). The blue data points (expanded view in the inset) were obtained in the absence of PAA, whereby detection of  $\text{HNO}_3$  at  $m/z$  62 is inefficient. The error bars are  $1\sigma$  statistical uncertainty in the signal at  $m/z$  62 and 17 % total uncertainty in the  $\text{HNO}_3$  mixing ratio. (b) Change in normalised signals at  $m/z$  62 and  $m/z$  59 upon adding  $\text{HNO}_3$  for the same dataset (i.e. background corrected signals). The error bars are  $1\sigma$  statistical uncertainty.

635

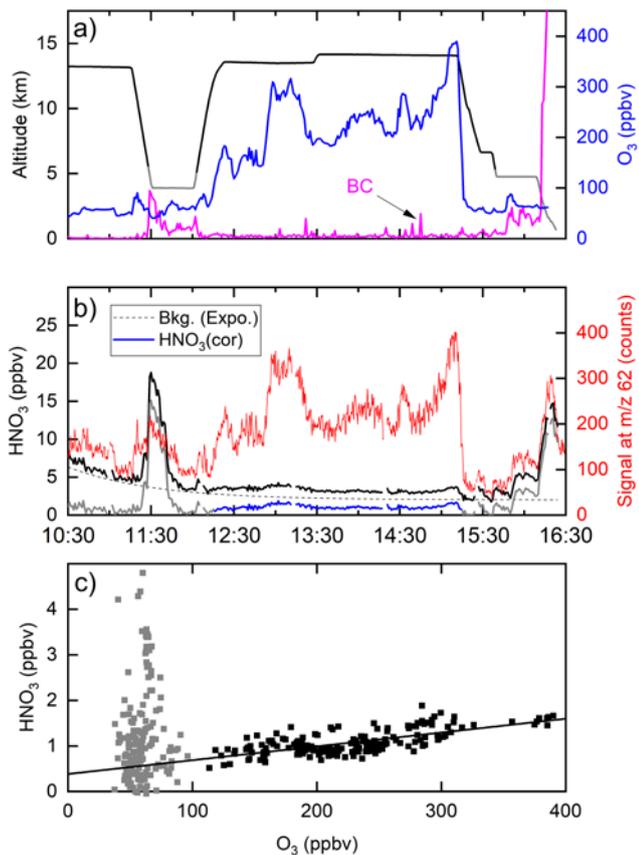


**Figure 10.** a) Altitude (black) and O<sub>3</sub> mixing ratios (blue) from a HALO-flight during the CAFE-Africa campaign. The purple line (arbitrary units) is proportional to the black-carbon particle number density (BC). b) The signal at  $m/z$  62 (red line) clearly co-varies with O<sub>3</sub>. Following conversion to a mixing ratio (black line) and subtraction of an HNO<sub>3</sub> background signal (dotted line, assuming an exponential decay) originating in the <sup>210</sup>Po-source, the solid blue line for HNO<sub>3</sub> is obtained (HNO<sub>3</sub> cor). c) HNO<sub>3</sub> mixing ratios plotted versus O<sub>3</sub> mixing ratios. The straight black line has a slope of  $(3 \pm 0.5) \times 10^{-3}$  and does not take into account the grey data points (O<sub>3</sub> mixing ratio < 100 ppbv).

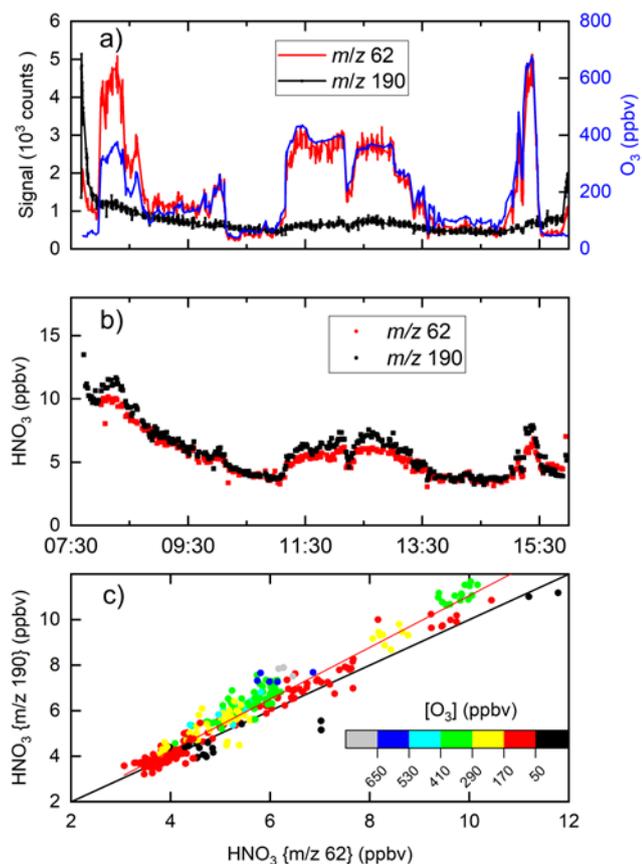


**Figure 11.** I-CIMS HNO<sub>3</sub> measurements and auxiliary data from a HALO-flight during the CAFE-EU campaign. a) Signals at *m/z* 62 and *m/z* 190 as well as O<sub>3</sub> mixing ratios. b) HNO<sub>3</sub> mixing ratios derived from the signals at *m/z* 62 and *m/z* 190 taking the dependence of sensitivity on ozone and relative humidity into account. c) Correlation of the HNO<sub>3</sub> mixing ratios derived from the two masses. The red line is a bivariate fit (slope 1.14 ± 0.05, intercept -0.3 ± 0.3), the black line is a 1:1 line. A large fraction of the HNO<sub>3</sub> measured stems from the polonium source, especially at the beginning of the flight.